Pion electromagnetic form factor from analyticity and unitarity

B. Ananthanarayan
Centre for High Energy Physics
Indian Institute of Science
Bangalore 560 012, India

work done in collaboration with
Irinel Caprini, Diganta Das and I. Sentitemsu Imsong

2015

Introduction

Introduction

The pion form factor

- encodes the information of strong interaction
- probe of perturbative QCD and asymptotic predictions
- enters the muon $(g-2)$ and other observables
- amenable to experiment in a variety of kinematic regimes
- spacelike ($t < 0$), timelike but analyticity region $0 < t < 4M_\pi^2$
- (physical) timelike region $t > 4M_\pi^2$ where it is complex
- analytic in the cut plane
- can be studied using general principles
- information is precise enough to test experiment in an essential way
- our work tests chiral perturbation theory and lattice
- produces a model independent determination (bounds) on the radius, shape parameters and modulus of the form factor in part of the spacelike region
- produces values for the two-pion contribution to the $(g-2)$ of the muon with central values agreeing with other determinations, but with reduced uncertainties

Based on the publications: BA, IC, DD and ISI, European Physical Journal, **C 72** (2012) 2192; **73** (2013) 2520; Physical Review **D 89** (2014) 036007.

Introduction

The pion form factor

- encodes the information of strong interaction
- probe of perturbative QCD and asymptotic predictions
- enters the muon $(g-2)$ and other observables
- amenable to experiment in a variety of kinematic regimes
- spacelike ($t < 0$), timelike but analyticity region $0 < t < 4M_\pi^2$
- (physical) timelike region $t > 4M_\pi^2$ where it is complex
- analytic in the cut plane
- can be studied using general principles
- information is precise enough to test experiment in an essential way
- our work tests chiral perturbation theory and lattice
- produces a model independent determination (bounds) on the radius, shape parameters and modulus of the form factor in part of the spacelike region
- produces values for the two-pion contribution to the $(g-2)$ of the muon with central values agreeing with other determinations, but with reduced uncertainties

Based on the publications: BA, IC, DD and ISI, European Physical Journal, **C 72** (2012) 2192; **73** (2013) 2520; Physical Review **D 89** (2014) 036007.

Introduction

The pion form factor

- encodes the information of strong interaction
- probe of perturbative QCD and asymptotic predictions
- enters the muon $(g-2)$ and other observables
- amenable to experiment in a variety of kinematic regimes
- spacelike ($t < 0$), timelike but analyticity region $0 < t < 4M_\pi^2$
- (physical) timelike region $t > 4M_\pi^2$ where it is complex
- analytic in the cut plane
- can be studied using general principles
- information is precise enough to test experiment in an essential way
- our work tests chiral perturbation theory and lattice
- produces a model independent determination (bounds) on the radius, shape parameters and modulus of the form factor in part of the spacelike region
- produces values for the two-pion contribution to the $(g-2)$ of the muon with central values agreeing with other determinations, but with reduced uncertainties

Based on the publications: BA, IC, DD and ISI, European Physical Journal, **C 72** (2012) 2192; **73** (2013) 2520; Physical Review **D 89** (2014) 036007.

Introduction

The pion form factor

- encodes the information of strong interaction
- probe of perturbative QCD and asymptotic predictions
- enters the muon $(g-2)$ and other observables
- amenable to experiment in a variety of kinematic regimes
- spacelike ($t<0$), timelike but analyticity region $0<t<4M_\pi^2$
- (physical) timelike region $t>4M_\pi^2$ where it is complex
- analytic in the cut plane
- can be studied using general principles
- information is precise enough to test experiment in an essential way
- our work tests chiral perturbation theory and lattice
- produces a model independent determination (bounds) on the radius, shape parameters and modulus of the form factor in part of the spacelike region
- produces values for the two-pion contribution to the $(g-2)$ of the muon with central values agreeing with other determinations, but with reduced uncertainties

Based on the publications: BA, IC, DD and ISI, European Physical Journal, **C 72** (2012) 2192; **73** (2013) 2520; Physical Review **D 89** (2014) 036007.

Introduction

The pion form factor

- encodes the information of strong interaction
- probe of perturbative QCD and asymptotic predictions
- enters the muon $(g-2)$ and other observables
- amenable to experiment in a variety of kinematic regimes
- spacelike ($t < 0$), timelike but analyticity region $0 < t < 4M_\pi^2$
- (physical) timelike region $t > 4M_\pi^2$ where it is complex
- analytic in the cut plane
- can be studied using general principles
- information is precise enough to test experiment in an essential way
- our work tests chiral perturbation theory and lattice
- produces a model independent determination (bounds) on the radius, shape parameters and modulus of the form factor in part of the spacelike region
- produces values for the two-pion contribution to the $(g-2)$ of the muon with central values agreeing with other determinations, but with reduced uncertainties

Based on the publications: BA, IC, DD and ISI, European Physical Journal, **C 72** (2012) 2192; **73** (2013) 2520; Physical Review **D 89** (2014) 036007.

The pion form factor

- encodes the information of strong interaction
- probe of perturbative QCD and asymptotic predictions
- enters the muon $(g-2)$ and other observables
- amenable to experiment in a variety of kinematic regimes
- spacelike ($t<0$), timelike but analyticity region $0<t<4M_\pi^2$
- (physical) timelike region $t>4M_\pi^2$ where it is complex
- analytic in the cut plane
- can be studied using general principles
- information is precise enough to test experiment in an essential way
- our work tests chiral perturbation theory and lattice
- produces a model independent determination (bounds) on the radius, shape parameters and modulus of the form factor in part of the spacelike region
- produces values for the two-pion contribution to the $(g-2)$ of the muon with central values agreeing with other determinations, but with reduced uncertainties

Based on the publications: BA, IC, DD and ISI, European Physical Journal, **C 72** (2012) 2192; **73** (2013) 2520; Physical Review **D 89** (2014) 036007.

Introduction

The pion form factor

- encodes the information of strong interaction
- probe of perturbative QCD and asymptotic predictions
- enters the muon $(g-2)$ and other observables
- amenable to experiment in a variety of kinematic regimes
- spacelike ($t<0$), timelike but analyticity region $0<t<4M_\pi^2$
- (physical) timelike region $t>4M_\pi^2$ where it is complex
- analytic in the cut plane
- can be studied using general principles
- information is precise enough to test experiment in an essential way
- our work tests chiral perturbation theory and lattice
- produces a model independent determination (bounds) on the radius, shape parameters and modulus of the form factor in part of the spacelike region
- produces values for the two-pion contribution to the $(g-2)$ of the muon with central values agreeing with other determinations, but with reduced uncertainties

Based on the publications: BA, IC, DD and ISI, European Physical Journal, **C 72** (2012) 2192; **73** (2013) 2520; Physical Review **D 89** (2014) 036007.

Introduction

The pion form factor

- encodes the information of strong interaction
- probe of perturbative QCD and asymptotic predictions
- enters the muon $(g-2)$ and other observables
- amenable to experiment in a variety of kinematic regimes
- spacelike ($t < 0$), timelike but analyticity region $0 < t < 4M_\pi^2$
- (physical) timelike region $t > 4M_\pi^2$ where it is complex
- analytic in the cut plane
- can be studied using general principles
- information is precise enough to test experiment in an essential way
- our work tests chiral perturbation theory and lattice
- produces a model independent determination (bounds) on the radius, shape parameters and modulus of the form factor in part of the spacelike region
- produces values for the two-pion contribution to the $(g-2)$ of the muon with central values agreeing with other determinations, but with reduced uncertainties

Based on the publications: BA, IC, DD and ISI, European Physical Journal, **C 72** (2012) 2192; **73** (2013) 2520; Physical Review **D 89** (2014) 036007.

Introduction

The pion form factor

- encodes the information of strong interaction
- probe of perturbative QCD and asymptotic predictions
- enters the muon $(g-2)$ and other observables
- amenable to experiment in a variety of kinematic regimes
- spacelike ($t < 0$), timelike but analyticity region $0 < t < 4M_\pi^2$
- (physical) timelike region $t > 4M_\pi^2$ where it is complex
- analytic in the cut plane
- can be studied using general principles
- information is precise enough to test experiment in an essential way
- our work tests chiral perturbation theory and lattice
- produces a model independent determination (bounds) on the radius, shape parameters and modulus of the form factor in part of the spacelike region
- produces values for the two-pion contribution to the $(g-2)$ of the muon with central values agreeing with other determinations, but with reduced uncertainties

Based on the publications: BA, IC, DD and ISI, European Physical Journal, **C 72** (2012) 2192; **73** (2013) 2520; Physical Review **D 89** (2014) 036007.

Introduction

The pion form factor

- encodes the information of strong interaction
- probe of perturbative QCD and asymptotic predictions
- enters the muon $(g-2)$ and other observables
- amenable to experiment in a variety of kinematic regimes
- spacelike ($t < 0$), timelike but analyticity region $0 < t < 4M_\pi^2$
- (physical) timelike region $t > 4M_\pi^2$ where it is complex
- analytic in the cut plane
- can be studied using general principles
- information is precise enough to test experiment in an essential way
- our work tests chiral perturbation theory and lattice
- produces a model independent determination (bounds) on the radius, shape parameters and modulus of the form factor in part of the spacelike region
- produces values for the two-pion contribution to the $(g-2)$ of the muon with central values agreeing with other determinations, but with reduced uncertainties

Based on the publications: BA, IC, DD and ISI, European Physical Journal, **C 72** (2012) 2192; **73** (2013) 2520; Physical Review **D 89** (2014) 036007.

Introduction

The pion form factor

- encodes the information of strong interaction
- probe of perturbative QCD and asymptotic predictions
- enters the muon $(g-2)$ and other observables
- amenable to experiment in a variety of kinematic regimes
- spacelike ($t < 0$), timelike but analyticity region $0 < t < 4M_\pi^2$
- (physical) timelike region $t > 4M_\pi^2$ where it is complex
- analytic in the cut plane
- can be studied using general principles
- information is precise enough to test experiment in an essential way
- our work tests chiral perturbation theory and lattice
- produces a model independent determination (bounds) on the radius, shape parameters and modulus of the form factor in part of the spacelike region
- produces values for the two-pion contribution to the $(g-2)$ of the muon with central values agreeing with other determinations, but with reduced uncertainties

Based on the publications: BA, IC, DD and ISI, European Physical Journal, **C 72** (2012) 2192; **73** (2013) 2520; Physical Review **D 89** (2014) 036007.

Introduction

The pion form factor

- encodes the information of strong interaction
- probe of perturbative QCD and asymptotic predictions
- enters the muon $(g-2)$ and other observables
- amenable to experiment in a variety of kinematic regimes
- spacelike ($t < 0$), timelike but analyticity region $0 < t < 4M_\pi^2$
- (physical) timelike region $t > 4M_\pi^2$ where it is complex
- analytic in the cut plane
- can be studied using general principles
- information is precise enough to test experiment in an essential way
- our work tests chiral perturbation theory and lattice
- produces a model independent determination (bounds) on the radius, shape parameters and modulus of the form factor in part of the spacelike region
- produces values for the two-pion contribution to the $(g-2)$ of the muon with central values agreeing with other determinations, but with reduced uncertainties

Based on the publications: BA, IC, DD and ISI, European Physical Journal, **C 72** (2012) 2192; **73** (2013) 2520; Physical Review **D 89** (2014) 036007.

Introduction

The pion form factor

- encodes the information of strong interaction
- probe of perturbative QCD and asymptotic predictions
- enters the muon $(g-2)$ and other observables
- amenable to experiment in a variety of kinematic regimes
- spacelike ($t < 0$), timelike but analyticity region $0 < t < 4M_\pi^2$
- (physical) timelike region $t > 4M_\pi^2$ where it is complex
- analytic in the cut plane
- can be studied using general principles
- information is precise enough to test experiment in an essential way
- our work tests chiral perturbation theory and lattice
- produces a model independent determination (bounds) on the radius, shape parameters and modulus of the form factor in part of the spacelike region
- produces values for the two-pion contribution to the $(g-2)$ of the muon with central values agreeing with other determinations, but with reduced uncertainties

Based on the publications: BA, IC, DD and ISI, European Physical Journal, **C 72** (2012) 2192; **73** (2013) 2520; Physical Review **D 89** (2014) 036007.

Introduction

The pion form factor

- encodes the information of strong interaction
- probe of perturbative QCD and asymptotic predictions
- enters the muon $(g-2)$ and other observables
- amenable to experiment in a variety of kinematic regimes
- spacelike ($t<0$), timelike but analyticity region $0<t<4M_\pi^2$
- (physical) timelike region $t>4M_\pi^2$ where it is complex
- analytic in the cut plane
- can be studied using general principles
- information is precise enough to test experiment in an essential way
- our work tests chiral perturbation theory and lattice
- produces a model independent determination (bounds) on the radius, shape parameters and modulus of the form factor in part of the spacelike region
- produces values for the two-pion contribution to the $(g-2)$ of the muon with central values agreeing with other determinations, but with reduced uncertainties

Based on the publications: BA, IC, DD and ISI, European Physical Journal, **C 72** (2012) 2192; **73** (2013) 2520; Physical Review **D 89** (2014) 036007.

Strategy

- Model independent method to optimize inputs coming from various sources
- Phase shift in the elastic region now known to great accuracy
- Modulus information known from high statistics experiments in the elastic region, in regions of stability where experiments essentially agree
- Measurements in the spacelike region
- Framework that results from completely general principles
- Theory of complex variables as the building block
- Using analyticity to correlate all these inputs without dangers of instabilities
- Outcome: reliable bounds for the radius, shape parameters, bounds on modulus in low energy region where data are either scarce or in conflict, and saturation of the integral for muon $g-2$, with the possibility of reduced error, using the results in a self-consistent manner
- Our central values are consistent with prior determinations, but the error we attach is lowered compared to other determinations, due to the correlation introduced by analyticity and unitarity

Strategy

- Model independent method to optimize inputs coming from various sources
- Phase shift in the elastic region now known to great accuracy
- Modulus information known from high statistics experiments in the elastic region, in regions of stability where experiments essentially agree
- Measurements in the spacelike region
- Framework that results from completely general principles
- Theory of complex variables as the building block
- Using analyticity to correlate all these inputs without dangers of instabilities
- Outcome: reliable bounds for the radius, shape parameters, bounds on modulus in low energy region where data are either scarce or in conflict, and saturation of the integral for muon $g-2$, with the possibility of reduced error, using the results in a self-consistent manner
- Our central values are consistent with prior determinations, but the error we attach is lowered compared to other determinations, due to the correlation introduced by analyticity and unitarity

Strategy

- Model independent method to optimize inputs coming from various sources
- Phase shift in the elastic region now known to great accuracy
- Modulus information known from high statistics experiments in the elastic region, in regions of stability where experiments essentially agree
- Measurements in the spacelike region
- Framework that results from completely general principles
- Theory of complex variables as the building block
- Using analyticity to correlate all these inputs without dangers of instabilities
- Outcome: reliable bounds for the radius, shape parameters, bounds on modulus in low energy region where data are either scarce or in conflict, and saturation of the integral for muon $g-2$, with the possibility of reduced error, using the results in a self-consistent manner
- Our central values are consistent with prior determinations, but the error we attach is lowered compared to other determinations, due to the correlation introduced by analyticity and unitarity

Strategy

- Model independent method to optimize inputs coming from various sources
- Phase shift in the elastic region now known to great accuracy
- Modulus information known from high statistics experiments in the elastic region, in regions of stability where experiments essentially agree
- Measurements in the spacelike region
- Framework that results from completely general principles
- Theory of complex variables as the building block
- Using analyticity to correlate all these inputs without dangers of instabilities
- Outcome: reliable bounds for the radius, shape parameters, bounds on modulus in low energy region where data are either scarce or in conflict, and saturation of the integral for muon $g-2$, with the possibility of reduced error, using the results in a self-consistent manner
- Our central values are consistent with prior determinations, but the error we attach is lowered compared to other determinations, due to the correlation introduced by analyticity and unitarity

Strategy

- Model independent method to optimize inputs coming from various sources
- Phase shift in the elastic region now known to great accuracy
- Modulus information known from high statistics experiments in the elastic region, in regions of stability where experiments essentially agree
- Measurements in the spacelike region
- Framework that results from completely general principles
- Theory of complex variables as the building block
- Using analyticity to correlate all these inputs without dangers of instabilities
- Outcome: reliable bounds for the radius, shape parameters, bounds on modulus in low energy region where data are either scarce or in conflict, and saturation of the integral for muon $g-2$, with the possibility of reduced error, using the results in a self-consistent manner
- Our central values are consistent with prior determinations, but the error we attach is lowered compared to other determinations, due to the correlation introduced by analyticity and unitarity

Strategy

- Model independent method to optimize inputs coming from various sources
- Phase shift in the elastic region now known to great accuracy
- Modulus information known from high statistics experiments in the elastic region, in regions of stability where experiments essentially agree
- Measurements in the spacelike region
- Framework that results from completely general principles
- Theory of complex variables as the building block
- Using analyticity to correlate all these inputs without dangers of instabilities
- Outcome: reliable bounds for the radius, shape parameters, bounds on modulus in low energy region where data are either scarce or in conflict, and saturation of the integral for muon $g-2$, with the possibility of reduced error, using the results in a self-consistent manner
- Our central values are consistent with prior determinations, but the error we attach is lowered compared to other determinations, due to the correlation introduced by analyticity and unitarity

Strategy

- Model independent method to optimize inputs coming from various sources
- Phase shift in the elastic region now known to great accuracy
- Modulus information known from high statistics experiments in the elastic region, in regions of stability where experiments essentially agree
- Measurements in the spacelike region
- Framework that results from completely general principles
- Theory of complex variables as the building block
- Using analyticity to correlate all these inputs without dangers of instabilities
- Outcome: reliable bounds for the radius, shape parameters, bounds on modulus in low energy region where data are either scarce or in conflict, and saturation of the integral for muon $g-2$, with the possibility of reduced error, using the results in a self-consistent manner
- Our central values are consistent with prior determinations, but the error we attach is lowered compared to other determinations, due to the correlation introduced by analyticity and unitarity

Strategy

- Model independent method to optimize inputs coming from various sources
- Phase shift in the elastic region now known to great accuracy
- Modulus information known from high statistics experiments in the elastic region, in regions of stability where experiments essentially agree
- Measurements in the spacelike region
- Framework that results from completely general principles
- Theory of complex variables as the building block
- Using analyticity to correlate all these inputs without dangers of instabilities
- Outcome: reliable bounds for the radius, shape parameters, bounds on modulus in low energy region where data are either scarce or in conflict, and saturation of the integral for muon $g-2$, with the possibility of reduced error, using the results in a self-consistent manner
- Our central values are consistent with prior determinations, but the error we attach is lowered compared to other determinations, due to the correlation introduced by analyticity and unitarity

Strategy

- Model independent method to optimize inputs coming from various sources
- Phase shift in the elastic region now known to great accuracy
- Modulus information known from high statistics experiments in the elastic region, in regions of stability where experiments essentially agree
- Measurements in the spacelike region
- Framework that results from completely general principles
- Theory of complex variables as the building block
- Using analyticity to correlate all these inputs without dangers of instabilities
- Outcome: reliable bounds for the radius, shape parameters, bounds on modulus in low energy region where data are either scarce or in conflict, and saturation of the integral for muon $g-2$, with the possibility of reduced error, using the results in a self-consistent manner
- Our central values are consistent with prior determinations, but the error we attach is lowered compared to other determinations, due to the correlation introduced by analyticity and unitarity

Strategy

- Model independent method to optimize inputs coming from various sources
- Phase shift in the elastic region now known to great accuracy
- Modulus information known from high statistics experiments in the elastic region, in regions of stability where experiments essentially agree
- Measurements in the spacelike region
- Framework that results from completely general principles
- Theory of complex variables as the building block
- Using analyticity to correlate all these inputs without dangers of instabilities
- Outcome: reliable bounds for the radius, shape parameters, bounds on modulus in low energy region where data are either scarce or in conflict, and saturation of the integral for muon $g-2$, with the possibility of reduced error, using the results in a self-consistent manner
- Our central values are consistent with prior determinations, but the error we attach is lowered compared to other determinations, due to the correlation introduced by analyticity and unitarity

Definition and properties.

- Pion electromagnetic form factor $F(t)$ is defined as,

$$\langle \pi^+(p')| J_\mu^{\text{em}} |\pi^+(p)\rangle = (p+p')F_\pi(t), \quad t = q^2 = -Q^2 = (p-p')^2.$$

- $F_\pi(t)$ is normalized as $F_\pi(0) = 1$.
- $F_\pi(t)$ is real for $t \leq 4M_\pi^2$.
- branch cut from threshold of two particle production $t_+ = 4M_\pi^2$ to $t = \infty$.
- elastic region is $t_+ \leq t \leq t_{\text{in}}$, where $t_{\text{in}} = (M_\omega + M_{\pi^0})^2$ is the first inelastic threshold of $\omega\pi$ production. (dictated by phenomenology: theoretically given by $16M_\pi^2$)
- the expansion of the pion electromagnetic form factor around $t = 0$ is written as,

$$F_\pi(t) = 1 + \frac{1}{6} r_\pi^2 t + ct^2 + dt^3 + \cdots$$

Definition and properties.

- Pion electromagnetic form factor $F(t)$ is defined as,

$$\langle \pi^+(p') | J_\mu^{\text{em}} | \pi^+(p) \rangle = (p+p')F_\pi(t), \quad t = q^2 = -Q^2 = (p-p')^2.$$

- $F_\pi(t)$ is normalized as $F_\pi(0) = 1$.
- $F_\pi(t)$ is real for $t \leq 4M_\pi^2$.
- branch cut from threshold of two particle production $t_+ = 4M_\pi^2$ to $t = \infty$.
- elastic region is $t_+ \leq t \leq t_{\text{in}}$, where $t_{\text{in}} = (M_\omega + M_{\pi^0})^2$ is the first inelastic threshold of $\omega\pi$ production. (dictated by phenomenology: theoretically given by $16M_\pi^2$)
- the expansion of the pion electromagnetic form factor around $t = 0$ is written as,

$$F_\pi(t) = 1 + \frac{1}{6} r_\pi^2 t + ct^2 + dt^3 + \cdots$$

Definition and properties.

- Pion electromagnetic form factor $F(t)$ is defined as,

$$\langle \pi^+(p') |\, J_\mu^{\text{em}} \,| \pi^+(p) \rangle = (p+p')F_\pi(t), \quad t = q^2 = -Q^2 = (p-p')^2.$$

- $F_\pi(t)$ is normalized as $F_\pi(0) = 1$.
- $F_\pi(t)$ is real for $t \leq 4M_\pi^2$.
- branch cut from threshold of two particle production $t_+ = 4M_\pi^2$ to $t = \infty$.
- elastic region is $t_+ \leq t \leq t_{\text{in}}$, where $t_{\text{in}} = (M_\omega + M_{\pi^0})^2$ is the first inelastic threshold of $\omega\pi$ production. (dictated by phenomenology: theoretically given by $16M_\pi^2$)
- the expansion of the pion electromagnetic form factor around $t = 0$ is written as,

$$F_\pi(t) = 1 + \frac{1}{6} r_\pi^2 t + ct^2 + dt^3 + \cdots$$

- Pion electromagnetic form factor $F(t)$ is defined as,

$$\langle \pi^+(p')| J_\mu^{\text{em}} |\pi^+(p)\rangle = (p+p')F_\pi(t), \quad t = q^2 = -Q^2 = (p-p')^2.$$

- $F_\pi(t)$ is normalized as $F_\pi(0) = 1$.
- $F_\pi(t)$ is real for $t \leq 4M_\pi^2$.
- branch cut from threshold of two particle production $t_+ = 4M_\pi^2$ to $t = \infty$.
- elastic region is $t_+ \leq t \leq t_{\text{in}}$, where $t_{\text{in}} = (M_\omega + M_{\pi^0})^2$ is the first inelastic threshold of $\omega\pi$ production. (dictated by phenomenology: theoretically given by $16M_\pi^2$)
- the expansion of the pion electromagnetic form factor around $t = 0$ is written as,

$$F_\pi(t) = 1 + \frac{1}{6}r_\pi^2 t + ct^2 + dt^3 + \cdots$$

- Pion electromagnetic form factor $F(t)$ is defined as,

$$\left\langle \pi^+(p')\right| J_\mu^{\text{em}} \left|\pi^+(p)\right\rangle = (p+p')F_\pi(t), \quad t = q^2 = -Q^2 = (p-p')^2.$$

- $F_\pi(t)$ is normalized as $F_\pi(0) = 1$.
- $F_\pi(t)$ is real for $t \leq 4M_\pi^2$.
- branch cut from threshold of two particle production $t_+ = 4M_\pi^2$ to $t = \infty$.
- elastic region is $t_+ \leq t \leq t_{\text{in}}$, where $t_{\text{in}} = (M_\omega + M_{\pi^0})^2$ is the first inelastic threshold of $\omega\pi$ production. (dictated by phenomenology: theoretically given by $16M_\pi^2$)
- the expansion of the pion electromagnetic form factor around $t = 0$ is written as,

$$F_\pi(t) = 1 + \frac{1}{6} r_\pi^2 t + ct^2 + dt^3 + \cdots$$

- Pion electromagnetic form factor $F(t)$ is defined as,

$$\langle \pi^+(p') | J_\mu^{\text{em}} | \pi^+(p) \rangle = (p+p')F_\pi(t), \quad t = q^2 = -Q^2 = (p-p')^2.$$

- $F_\pi(t)$ is normalized as $F_\pi(0) = 1$.
- $F_\pi(t)$ is real for $t \leq 4M_\pi^2$.
- branch cut from threshold of two particle production $t_+ = 4M_\pi^2$ to $t = \infty$.
- elastic region is $t_+ \leq t \leq t_{\text{in}}$, where $t_{\text{in}} = (M_\omega + M_{\pi^0})^2$ is the first inelastic threshold of $\omega\pi$ production. (dictated by phenomenology: theoretically given by $16M_\pi^2$)
- the expansion of the pion electromagnetic form factor around $t = 0$ is written as,

$$F_\pi(t) = 1 + \frac{1}{6} r_\pi^2 t + ct^2 + dt^3 + \cdots$$

Definition and properties.

- Pion electromagnetic form factor $F(t)$ is defined as,

$$\left\langle \pi^+(p') \right| J_\mu^{\text{em}} \left| \pi^+(p) \right\rangle = (p+p')F_\pi(t), \quad t = q^2 = -Q^2 = (p-p')^2.$$

- $F_\pi(t)$ is normalized as $F_\pi(0) = 1$.
- $F_\pi(t)$ is real for $t \leq 4M_\pi^2$.
- branch cut from threshold of two particle production $t_+ = 4M_\pi^2$ to $t = \infty$.
- elastic region is $t_+ \leq t \leq t_{\text{in}}$, where $t_{\text{in}} = (M_\omega + M_{\pi^0})^2$ is the first inelastic threshold of $\omega\pi$ production. (dictated by phenomenology: theoretically given by $16M_\pi^2$)
- the expansion of the pion electromagnetic form factor around $t = 0$ is written as,

$$F_\pi(t) = 1 + \frac{1}{6} r_\pi^2 t + ct^2 + dt^3 + \cdots$$

Theory Descriptions.

- At large spacelike momenta $Q^2 = -t > 0$, perturbative QCD predicts at LO, [Lepage & Brodsky 1979, Efremov & Radyushkin 1980, Farrar & Jackson 1979]

$$F_\pi(-Q^2) \sim \frac{16\pi f_\pi^2 \alpha_s(Q^2)}{Q^2}, \qquad Q^2 \to \infty,$$

where, f_π is the pion decay constant.

- asymptotic behavior for large time like momenta $t > 0$ [Cornille & Martin, 1975]

$$|F_\pi(t)| \sim \frac{1}{t}.$$

- Low energy description: ChPT up to two loops [Gasser & Meissner 1991, Colangelo, Finkemeier & Urech 1996, Bijnens, Colangelo & Talavera 1998]
- Lattice gauge theory [Aoki *et. al* 2009]

Theory Descriptions.

- At large spacelike momenta $Q^2 = -t > 0$, perturbative QCD predicts at LO, [Lepage & Brodsky 1979, Efremov & Radyushkin 1980, Farrar & Jackson 1979]

$$F_\pi(-Q^2) \sim \frac{16\pi f_\pi^2 \alpha_s(Q^2)}{Q^2}, \qquad Q^2 \to \infty,$$

where, f_π is the pion decay constant.

- asymptotic behavior for large time like momenta $t > 0$ [Cornille & Martin, 1975]

$$|F_\pi(t)| \sim \frac{1}{t}.$$

- Low energy description: ChPT up to two loops [Gasser & Meissner 1991, Colangelo, Finkemeier & Urech 1996, Bijnens, Colangelo & Talavera 1998]
- Lattice gauge theory [Aoki *et. al* 2009]

Theory Descriptions.

- At large spacelike momenta $Q^2 = -t > 0$, perturbative QCD predicts at LO, [Lepage & Brodsky 1979, Efremov & Radyushkin 1980, Farrar & Jackson 1979]

$$F_\pi(-Q^2) \sim \frac{16\pi f_\pi^2 \alpha_s(Q^2)}{Q^2}, \qquad Q^2 \to \infty,$$

where, f_π is the pion decay constant.

- asymptotic behavior for large time like momenta $t > 0$ [Cornille & Martin, 1975]

$$|F_\pi(t)| \sim \frac{1}{t}.$$

- Low energy description: ChPT up to two loops [Gasser & Meissner 1991, Colangelo, Finkemeier & Urech 1996, Bijnens, Colangelo & Talavera 1998]
- Lattice gauge theory [Aoki *et. al* 2009]

Theory Descriptions.

- At large spacelike momenta $Q^2 = -t > 0$, perturbative QCD predicts at LO, [Lepage & Brodsky 1979, Efremov & Radyushkin 1980, Farrar & Jackson 1979]

$$F_\pi(-Q^2) \sim \frac{16\pi f_\pi^2 \alpha_s(Q^2)}{Q^2}, \qquad Q^2 \to \infty,$$

  where, f_π is the pion decay constant.
- asymptotic behavior for large time like momenta $t > 0$ [Cornille & Martin, 1975]

$$|F_\pi(t)| \sim \frac{1}{t}.$$

- Low energy description: ChPT up to two loops [Gasser & Meissner 1991, Colangelo, Finkemeier & Urech 1996, Bijnens, Colangelo & Talavera 1998]
- Lattice gauge theory [Aoki *et. al* 2009]

Theory Descriptions.

- At large spacelike momenta $Q^2 = -t > 0$, perturbative QCD predicts at LO, [Lepage & Brodsky 1979, Efremov & Radyushkin 1980, Farrar & Jackson 1979]

$$F_\pi(-Q^2) \sim \frac{16\pi f_\pi^2 \alpha_s(Q^2)}{Q^2}, \qquad Q^2 \to \infty,$$

  where, f_π is the pion decay constant.
- asymptotic behavior for large time like momenta $t > 0$ [Cornille & Martin, 1975]

$$|F_\pi(t)| \sim \frac{1}{t}.$$

- Low energy description: ChPT up to two loops [Gasser & Meissner 1991, Colangelo, Finkemeier & Urech 1996, Bijnens, Colangelo & Talavera 1998]
- Lattice gauge theory [Aoki *et. al* 2009]

The Generalized Meiman problem

- If the phase of the form factor is known (from Fermi-Watson theorem in the elastic region from scattering)

$$\text{Arg}[F(t+i\epsilon)] = \delta_1^1, \quad t_+ \leq t \leq t_{in},$$

where δ_1^1 is the phase shift of the P-wave of $\pi\pi$ elastic scattering.

- If the modulus $|F(t)|$ known above t_{in}. The information on modulus is used to obtain a reliable evaluation of

$$\frac{1}{\pi}\int_{t_{in}}^{\infty} dt \rho(t)|F_\pi(t)|^2 = I.$$

- with $\rho(t)$ are the weight functions of the following type

$$\rho(t) = \frac{t^\beta}{(t+Q^2)^\gamma},$$

where, $Q^2 \geq 0$ and β and γ satisfy the relation $\beta \leq \gamma \leq \beta + 2$ (to ensure convergence)

- *problem is to find constraints on the values $F(t)$ and its derivatives outside the cut* [Meiman, 1963, Duren, 1970]
- Many early applications: [Okubo, 1970, Micu, 1972, Auberson, 1975, Singh & Raina, 1979]

- If the phase of the form factor is known (from Fermi-Watson theorem in the elastic region from scattering)

$$\text{Arg}[F(t+i\epsilon)] = \delta_1^1, \quad t_+ \leq t \leq t_{in},$$

where δ_1^1 is the phase shift of the P-wave of $\pi\pi$ elastic scattering.

- If the modulus $|F(t)|$ known above $t_{\rm in}$. The information on modulus is used to obtain a reliable evaluation of

$$\frac{1}{\pi}\int_{t_{in}}^{\infty} dt \rho(t)|F_\pi(t)|^2 = I.$$

- with $\rho(t)$ are the weight functions of the following type

$$\rho(t) = \frac{t^\beta}{(t+Q^2)^\gamma},$$

where, $Q^2 \geq 0$ and β and γ satisfy the relation $\beta \leq \gamma \leq \beta + 2$ (to ensure convergence)

- *problem is to find constraints on the values $F(t)$ and its derivatives outside the cut* [Meiman, 1963, Duren, 1970]
- Many early applications: [Okubo, 1970, Micu, 1972, Auberson, 1975, Singh & Raina, 1979]

Generalized Meiman Problem

- If the phase of the form factor is known (from Fermi-Watson theorem in the elastic region from scattering)

$$\text{Arg}[F(t+i\epsilon)] = \delta_1^1, \quad t_+ \leq t \leq t_{in},$$

where δ_1^1 is the phase shift of the P-wave of $\pi\pi$ elastic scattering.

- If the modulus $|F(t)|$ known above $t_{\rm in}$. The information on modulus is used to obtain a reliable evaluation of

$$\frac{1}{\pi}\int_{t_{in}}^{\infty} dt \rho(t)|F_\pi(t)|^2 = I.$$

- with $\rho(t)$ are the weight functions of the following type

$$\rho(t) = \frac{t^\beta}{(t+Q^2)^\gamma},$$

where, $Q^2 \geq 0$ and β and γ satisfy the relation $\beta \leq \gamma \leq \beta + 2$ (to ensure convergence)

- *problem is to find constraints on the values $F(t)$ and its derivatives outside the cut* [Meiman, 1963, Duren, 1970]
- Many early applications: [Okubo, 1970, Micu, 1972, Auberson, 1975, Singh & Raina, 1979]

Generalized Meiman Problem

- If the phase of the form factor is known (from Fermi-Watson theorem in the elastic region from scattering)

$$\text{Arg}[F(t+i\epsilon)] = \delta_1^1, \quad t_+ \le t \le t_{in},$$

where δ_1^1 is the phase shift of the P-wave of $\pi\pi$ elastic scattering.

- If the modulus $|F(t)|$ known above t_{in}. The information on modulus is used to obtain a reliable evaluation of

$$\frac{1}{\pi}\int_{t_{in}}^{\infty} dt\rho(t)|F_\pi(t)|^2 = I.$$

- with $\rho(t)$ are the weight functions of the following type

$$\rho(t) = \frac{t^\beta}{(t+Q^2)^\gamma},$$

where, $Q^2 \ge 0$ and β and γ satisfy the relation $\beta \le \gamma \le \beta + 2$ (to ensure convergence)

- *problem is to find constraints on the values $F(t)$ and its derivatives outside the cut* [Meiman, 1963, Duren, 1970]
- Many early applications: [Okubo, 1970, Micu, 1972, Auberson, 1975, Singh & Raina, 1979]

Generalized Meiman Problem

- If the phase of the form factor is known (from Fermi-Watson theorem in the elastic region from scattering)

$$\text{Arg}[F(t+i\epsilon)] = \delta_1^1, \quad t_+ \leq t \leq t_{in},$$

where δ_1^1 is the phase shift of the P-wave of $\pi\pi$ elastic scattering.

- If the modulus $|F(t)|$ known above t_{in}. The information on modulus is used to obtain a reliable evaluation of

$$\frac{1}{\pi}\int_{t_{in}}^{\infty} dt\rho(t)|F_\pi(t)|^2 = I.$$

- with $\rho(t)$ are the weight functions of the following type

$$\rho(t) = \frac{t^\beta}{(t+Q^2)^\gamma},$$

where, $Q^2 \geq 0$ and β and γ satisfy the relation $\beta \leq \gamma \leq \beta + 2$ (to ensure convergence)

- *problem is to find constraints on the values $F(t)$ and its derivatives outside the cut* [Meiman, 1963, Duren, 1970]
- Many early applications: [Okubo, 1970, Micu, 1972, Auberson, 1975, Singh & Raina, 1979]

Generalized Meiman Problem

- If the phase of the form factor is known (from Fermi-Watson theorem in the elastic region from scattering)

$$\text{Arg}[F(t+i\epsilon)] = \delta_1^1, \quad t_+ \leq t \leq t_{in},$$

where δ_1^1 is the phase shift of the P-wave of $\pi\pi$ elastic scattering.

- If the modulus $|F(t)|$ known above $t_{\rm in}$. The information on modulus is used to obtain a reliable evaluation of

$$\frac{1}{\pi}\int_{t_{in}}^{\infty} dt \rho(t) |F_\pi(t)|^2 = I.$$

- with $\rho(t)$ are the weight functions of the following type

$$\rho(t) = \frac{t^\beta}{(t+Q^2)^\gamma},$$

where, $Q^2 \geq 0$ and β and γ satisfy the relation $\beta \leq \gamma \leq \beta + 2$ (to ensure convergence)

- *problem is to find constraints on the values $F(t)$ and its derivatives outside the cut* [Meiman, 1963, Duren, 1970]
- Many early applications: [Okubo, 1970, Micu, 1972, Auberson, 1975, Singh & Raina, 1979]

Generalized problem

- The phase information along $t_+ \leq t \leq t_{in}$ is taken into account by defining the Omnès function,[Caprini 2000]

$$\mathcal{O}(t) = \exp\Big(\frac{t}{\pi}\int_{t_+}^{\infty} dt' \, \frac{\delta(t')}{t'(t'-t)}\Big)$$

  where, $\delta(t) = \delta_1^1(t)$ for $t \leq t_{\text{in}}$, and is Lipschitz continuous for $t \geq t_{\text{in}}$.
- Using Omnès function $F_\pi(t)$ can be written as,

$$F_\pi(t) = \mathcal{O}(t)h(t)$$

  such that, $h(t)$ is real for $t \leq t_{\text{in}}$, *i.e.* it is analytic in the t-plane cut along $t > t_{\text{in}}$.
- the integral condition reads as,

$$\frac{1}{\pi}\int_{t_{\text{in}}}^{\infty} dt \rho(t)|\mathcal{O}(t)|^2 |h(t)|^2 = I$$

- The phase information along $t_+ \leq t \leq t_{in}$ is taken into account by defining the Omnès function,[Caprini 2000]

$$\mathcal{O}(t) = \exp\Big(\frac{t}{\pi}\int_{t_+}^{\infty} dt' \frac{\delta(t')}{t'(t'-t)}\Big)$$

where, $\delta(t) = \delta_1^1(t)$ for $t \leq t_{\text{in}}$, and is Lipschitz continuous for $t \geq t_{\text{in}}$.

- Using Omnès function $F_\pi(t)$ can be written as,

$$F_\pi(t) = \mathcal{O}(t)h(t)$$

such that, $h(t)$ is real for $t \leq t_{\text{in}}$, *i.e.* it is analytic in the t-plane cut along $t > t_{\text{in}}$.

- the integral condition reads as,

$$\frac{1}{\pi}\int_{t_{\text{in}}}^{\infty} dt \rho(t)|\mathcal{O}(t)|^2|h(t)|^2 = I$$

Generalized problem

- The phase information along $t_+ \leq t \leq t_{in}$ is taken into account by defining the Omnès function,[Caprini 2000]

$$\mathcal{O}(t) = \exp\Big(\frac{t}{\pi}\int_{t_+}^{\infty} dt' \frac{\delta(t')}{t'(t'-t)}\Big)$$

where, $\delta(t) = \delta_1^1(t)$ for $t \leq t_{\text{in}}$, and is Lipschitz continuous for $t \geq t_{\text{in}}$.

- Using Omnès function $F_\pi(t)$ can be written as,

$$F_\pi(t) = \mathcal{O}(t)h(t)$$

such that, $h(t)$ is real for $t \leq t_{\text{in}}$, *i.e.* it is analytic in the t-plane cut along $t > t_{\text{in}}$.

- the integral condition reads as,

$$\frac{1}{\pi}\int_{t_{\text{in}}}^{\infty} dt \rho(t)|\mathcal{O}(t)|^2|h(t)|^2 = I$$

- The phase information along $t_+ \leq t \leq t_{in}$ is taken into account by defining the Omnès function,[Caprini 2000]

$$\mathcal{O}(t) = \exp\Big(\frac{t}{\pi}\int_{t_+}^{\infty} dt' \frac{\delta(t')}{t'(t'-t)}\Big)$$

where, $\delta(t) = \delta_1^1(t)$ for $t \leq t_{\text{in}}$, and is Lipschitz continuous for $t \geq t_{\text{in}}$.

- Using Omnès function $F_\pi(t)$ can be written as,

$$F_\pi(t) = \mathcal{O}(t)h(t)$$

such that, $h(t)$ is real for $t \leq t_{\text{in}}$, *i.e.* it is analytic in the t-plane cut along $t > t_{\text{in}}$.

- the integral condition reads as,

$$\frac{1}{\pi}\int_{t_{\text{in}}}^{\infty} dt\rho(t)|\mathcal{O}(t)|^2|h(t)|^2 = I$$

Conformal Map

- the problem is cast into a canonical form by performing a conformal transformation,

$$\tilde{z} = \frac{\sqrt{t_{\text{in}}} - \sqrt{t_{\text{in}} - t}}{\sqrt{t_{\text{in}}} + \sqrt{t_{\text{in}} - t}}$$

  the transformation maps the complex t-plane cut for $t > t_{in}$ onto the unit disk $|z| < 1$ in the z-plane defined by $z \equiv \tilde{z}(t)$.

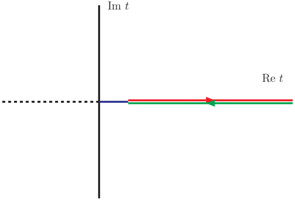

- The upper (lower) lip of the branch-cut $[t_{\text{in}}, \infty]$ is mapped onto the upper (lower) half of the unit circle in the complex z-plane,
- the real line $[-\infty, 0]$ to $[-1, 0]$ and $[0, t_{\text{in}}]$ to $[0, 1]$.

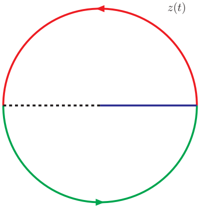

Conformal Map

- the problem is cast into a canonical form by performing a conformal transformation,

$$\tilde{z} = \frac{\sqrt{t_{\text{in}}} - \sqrt{t_{\text{in}} - t}}{\sqrt{t_{\text{in}}} + \sqrt{t_{\text{in}} - t}}$$

  the transformation maps the complex t-plane cut for $t > t_{in}$ onto the unit disk $|z| < 1$ in the z-plane defined by $z \equiv \tilde{z}(t)$.

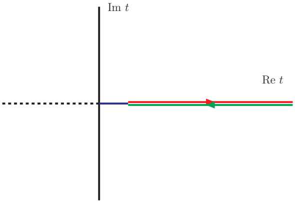

- The upper (lower) lip of the branch-cut $[t_{\text{in}}, \infty]$ is mapped onto the upper (lower) half of the unit circle in the complex z-plane,
- the real line $[-\infty, 0]$ to $[-1, 0]$ and $[0, t_{\text{in}}]$ to $[0, 1]$.

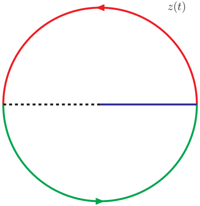

Conformal Map

- the problem is cast into a canonical form by performing a conformal transformation,

$$\tilde{z} = \frac{\sqrt{t_{\text{in}}} - \sqrt{t_{\text{in}} - t}}{\sqrt{t_{\text{in}}} + \sqrt{t_{\text{in}} - t}}$$

  the transformation maps the complex t-plane cut for $t > t_{in}$ onto the unit disk $|z| < 1$ in the z-plane defined by $z \equiv \tilde{z}(t)$.

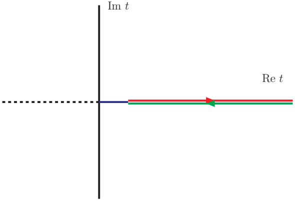

  - The upper (lower) lip of the branch-cut $[t_{\text{in}}, \infty]$ is mapped onto the upper (lower) half of the unit circle in the complex z-plane,
  - the real line $[-\infty, 0]$ to $[-1, 0]$ and $[0, t_{\text{in}}]$ to $[0, 1]$.

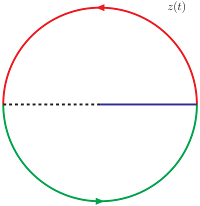

Determinantal Inequality

- using the conformal transformation, the integral condition can be written as,

$$\frac{1}{2\pi}\int_0^{2\pi} d\theta |g(e^{i\theta})|^2 = I, \quad z = e^{i\theta},$$

- we have defined $g(z) = w(z)\omega(z)F(\tilde{t}(z))[\mathcal{O}(\tilde{t}(z))]^{-1}$,
- $w(z)$ and $\omega(z)$ are the "outer functions" for the weight function and Jacobian of the transformation, and $|\mathcal{O}(t)|$ and are written as,

$$w(z) = (2\sqrt{t_{\rm in}})^{1+\beta-\gamma}\frac{(1-z)^{1/2}}{(1+z)^{3/2-\gamma+\beta}}\frac{(1+\tilde{z}(-Q^2))^{\gamma}}{(1-z\tilde{z}(-Q^2))^{\gamma}},$$

$$\omega(z) = \exp\left(\frac{\sqrt{t_{\rm in}-\tilde{t}(z)}}{\pi}\int_{t_{\rm in}}^{\infty}\frac{\ln|\mathcal{O}(t')|\,dt'}{\sqrt{t'-t_{\rm in}}(t'-\tilde{t}(z))}\right),$$

where $\tilde{t}(z)$ is the inverse of $z = \tilde{z}(t)$, for $\tilde{z}(t)$

- using the conformal transformation, the integral condition can be written as,

$$\frac{1}{2\pi}\int_0^{2\pi} d\theta |g(e^{i\theta})|^2 = I, \quad z = e^{i\theta},$$

- we have defined $g(z) = w(z)\omega(z)F(\tilde{t}(z))[\mathcal{O}(\tilde{t}(z))]^{-1}$,
- $w(z)$ and $\omega(z)$ are the “outer functions” for the weight function and Jacobian of the transformation, and $|\mathcal{O}(t)|$ and are written as,

$$w(z) = (2\sqrt{t_{\rm in}})^{1+\beta-\gamma}\frac{(1-z)^{1/2}}{(1+z)^{3/2-\gamma+\beta}}\frac{(1+\tilde{z}(-Q^2))^{\gamma}}{(1-z\tilde{z}(-Q^2))^{\gamma}},$$

$$\omega(z) = \exp\left(\frac{\sqrt{t_{\rm in}-\tilde{t}(z)}}{\pi}\int_{t_{\rm in}}^{\infty}\frac{\ln|\mathcal{O}(t')|\,{\rm d}t'}{\sqrt{t'-t_{\rm in}}(t'-\tilde{t}(z))}\right),$$

where $\tilde{t}(z)$ is the inverse of $z = \tilde{z}(t)$, for $\tilde{z}(t)$

Determinantal Inequality

- using the conformal transformation, the integral condition can be written as,

$$\frac{1}{2\pi}\int_0^{2\pi} d\theta |g(e^{i\theta})|^2 = I, \quad z = e^{i\theta},$$

- we have defined $g(z) = w(z)\omega(z)F(\tilde{t}(z))[\mathcal{O}(\tilde{t}(z))]^{-1}$,
- $w(z)$ and $\omega(z)$ are the "outer functions" for the weight function and Jacobian of the transformation, and $|\mathcal{O}(t)|$ and are written as,

$$w(z) = (2\sqrt{t_{\text{in}}})^{1+\beta-\gamma}\frac{(1-z)^{1/2}}{(1+z)^{3/2-\gamma+\beta}}\frac{(1+\tilde{z}(-Q^2))^{\gamma}}{(1-z\tilde{z}(-Q^2))^{\gamma}},$$

$$\omega(z) = \exp\left(\frac{\sqrt{t_{\text{in}}-\tilde{t}(z)}}{\pi}\int_{t_{\text{in}}}^{\infty}\frac{\ln|\mathcal{O}(t')|\,\mathrm{d}t'}{\sqrt{t'-t_{\text{in}}}(t'-\tilde{t}(z))}\right),$$

where $\tilde{t}(z)$ is the inverse of $z = \tilde{z}(t)$, for $\tilde{z}(t)$

- with techniques of complex analysis, it can be shown that Eq-(1) leads to determinantal inequality,

$$\begin{vmatrix} \bar{I} & \bar{\xi}_1 & \bar{\xi}_2 & \cdots & \bar{\xi}_N \\ \bar{\xi}_1 & \frac{z_1^{2K}}{1-z_1^2} & \frac{(z_1 z_2)^K}{1-z_1 z_2} & \cdots & \frac{(z_1 z_N)^K}{1-z_1 z_N} \\ \bar{\xi}_2 & \frac{(z_1 z_2)^K}{1-z_1 z_2} & \frac{(z_2)^{2K}}{1-z_2^2} & \cdots & \frac{(z_2 z_N)^K}{1-z_2 z_N} \\ \vdots & \vdots & \vdots & \vdots & \vdots \\ \bar{\xi}_N & \frac{(z_1 z_N)^K}{1-z_1 z_N} & \frac{(z_2 z_N)^K}{1-z_2 z_N} & \cdots & \frac{z_N^{2K}}{1-z_N^2} \end{vmatrix} \geq 0,$$

where the auxiliary quantities

$$\bar{I} = I - \sum_{k=0}^{K-1} g_k^2, \quad \bar{\xi}_n = g(z_n) - \sum_{k=0}^{K-1} g_k z_n^k$$

are defined in terms of the values :

$$\begin{aligned} \left[\frac{1}{k!}\frac{d^k g(z)}{dz^k}\right]_{z=0} &= g_k, \quad 0 \leq k \leq K-1, \\ g(z_n) &= \xi_n, \qquad 1 \leq n \leq N. \end{aligned}$$

- N real points $z_n \in (-1, 1)$ and $(K-1)$ derivatives at $z = 0$

Determinantal Inequality

- with techniques of complex analysis, it can be shown that Eq-(1) leads to determinantal inequality,

$$
\begin{vmatrix}
\bar{I} & \bar{\xi}_1 & \bar{\xi}_2 & \cdots & \bar{\xi}_N \\
\bar{\xi}_1 & \dfrac{z_1^{2K}}{1-z_1^2} & \dfrac{(z_1 z_2)^K}{1-z_1 z_2} & \cdots & \dfrac{(z_1 z_N)^K}{1-z_1 z_N} \\
\bar{\xi}_2 & \dfrac{(z_1 z_2)^K}{1-z_1 z_2} & \dfrac{(z_2)^{2K}}{1-z_2^2} & \cdots & \dfrac{(z_2 z_N)^K}{1-z_2 z_N} \\
\vdots & \vdots & \vdots & \vdots & \vdots \\
\bar{\xi}_N & \dfrac{(z_1 z_N)^K}{1-z_1 z_N} & \dfrac{(z_2 z_N)^K}{1-z_2 z_N} & \cdots & \dfrac{z_N^{2K}}{1-z_N^2}
\end{vmatrix} \geq 0,
$$

where the auxiliary quantities

$$
\bar{I} = I - \sum_{k=0}^{K-1} g_k^2, \quad \bar{\xi}_n = g(z_n) - \sum_{k=0}^{K-1} g_k z_n^k
$$

are defined in terms of the values :

$$
\begin{aligned}
\left[\frac{1}{k!}\frac{d^k g(z)}{dz^k}\right]_{z=0} &= g_k, \quad 0 \leq k \leq K-1, \\
g(z_n) &= \xi_n, \qquad 1 \leq n \leq N.
\end{aligned}
$$

- N real points $z_n \in (-1,1)$ and $(K-1)$ derivatives at $z=0$

Procedure

- In our evaluations, we supply the phase information to construct the Omnès function
- We construct the outer function for the Omnès function
- We construct the outer function for the weight and the Jacobian of the transformation
- We supply basic shape parameters, or alternatively constrain them by supplying information on the form factor from points in the (extended) analyticity region
- We obtain constraints on chosen points in the analyticity region by working the machinery
- Mathematically speaking there is no restriction on adding as many denumerable pieces of information as possible
- In practice experimental error begins to make the bounds lose coherence
- Small number of reliable experimental inputs are used

Procedure

- In our evaluations, we supply the phase information to construct the Omnès function
- We construct the outer function for the Omnès function
- We construct the outer function for the weight and the Jacobian of the transformation
- We supply basic shape parameters, or alternatively constrain them by supplying information on the form factor from points in the (extended) analyticity region
- We obtain constraints on chosen points in the analyticity region by working the machinery
- Mathematically speaking there is no restriction on adding as many denumerable pieces of information as possible
- In practice experimental error begins to make the bounds lose coherence
- Small number of reliable experimental inputs are used

Procedure

- In our evaluations, we supply the phase information to construct the Omnès function
- We construct the outer function for the Omnès function
- We construct the outer function for the weight and the Jacobian of the transformation
- We supply basic shape parameters, or alternatively constrain them by supplying information on the form factor from points in the (extended) analyticity region
- We obtain constraints on chosen points in the analyticity region by working the machinery
- Mathematically speaking there is no restriction on adding as many denumerable pieces of information as possible
- In practice experimental error begins to make the bounds lose coherence
- Small number of reliable experimental inputs are used

Procedure

- In our evaluations, we supply the phase information to construct the Omnès function
- We construct the outer function for the Omnès function
- We construct the outer function for the weight and the Jacobian of the transformation
- We supply basic shape parameters, or alternatively constrain them by supplying information on the form factor from points in the (extended) analyticity region
- We obtain constraints on chosen points in the analyticity region by working the machinery
- Mathematically speaking there is no restriction on adding as many denumerable pieces of information as possible
- In practice experimental error begins to make the bounds lose coherence
- Small number of reliable experimental inputs are used

Procedure

- In our evaluations, we supply the phase information to construct the Omnès function
- We construct the outer function for the Omnès function
- We construct the outer function for the weight and the Jacobian of the transformation
- We supply basic shape parameters, or alternatively constrain them by supplying information on the form factor from points in the (extended) analyticity region
- We obtain constraints on chosen points in the analyticity region by working the machinery
- Mathematically speaking there is no restriction on adding as many denumerable pieces of information as possible
- In practice experimental error begins to make the bounds lose coherence
- Small number of reliable experimental inputs are used

Procedure

- In our evaluations, we supply the phase information to construct the Omnès function
- We construct the outer function for the Omnès function
- We construct the outer function for the weight and the Jacobian of the transformation
- We supply basic shape parameters, or alternatively constrain them by supplying information on the form factor from points in the (extended) analyticity region
- We obtain constraints on chosen points in the analyticity region by working the machinery
- Mathematically speaking there is no restriction on adding as many denumerable pieces of information as possible
- In practice experimental error begins to make the bounds lose coherence
- Small number of reliable experimental inputs are used

Procedure

- In our evaluations, we supply the phase information to construct the Omnès function
- We construct the outer function for the Omnès function
- We construct the outer function for the weight and the Jacobian of the transformation
- We supply basic shape parameters, or alternatively constrain them by supplying information on the form factor from points in the (extended) analyticity region
- We obtain constraints on chosen points in the analyticity region by working the machinery
- Mathematically speaking there is no restriction on adding as many denumerable pieces of information as possible
- In practice experimental error begins to make the bounds lose coherence
- Small number of reliable experimental inputs are used

Procedure

- In our evaluations, we supply the phase information to construct the Omnès function
- We construct the outer function for the Omnès function
- We construct the outer function for the weight and the Jacobian of the transformation
- We supply basic shape parameters, or alternatively constrain them by supplying information on the form factor from points in the (extended) analyticity region
- We obtain constraints on chosen points in the analyticity region by working the machinery
- Mathematically speaking there is no restriction on adding as many denumerable pieces of information as possible
- In practice experimental error begins to make the bounds lose coherence
- Small number of reliable experimental inputs are used

Procedure

- In our evaluations, we supply the phase information to construct the Omnès function
- We construct the outer function for the Omnès function
- We construct the outer function for the weight and the Jacobian of the transformation
- We supply basic shape parameters, or alternatively constrain them by supplying information on the form factor from points in the (extended) analyticity region
- We obtain constraints on chosen points in the analyticity region by working the machinery
- Mathematically speaking there is no restriction on adding as many denumerable pieces of information as possible
- In practice experimental error begins to make the bounds lose coherence
- Small number of reliable experimental inputs are used

Basic Inputs

Phase Inputs

- phase is determined from Roy equation [Ananthanarayan, Colangelo, Gasser, Leutwyler 2001, Colangelo, Gasser, Leutwyler 2001, Kaminski, Pelaez, Ynduráin 2008, Garcia-Martin, Kaminski, Pelaez, Ruiz de Elvira, Ynduráin 2011]
- below $\sqrt{t_{\text{in}}} = 0.917\text{GeV}$ the phase $\delta_1^1(t)$ is parametrized as,

$$\cot\delta_1^1(t) = \frac{\sqrt{t}}{2k^3}(M_\rho^2 - t)\left(\frac{2M_\pi^3}{M_\rho^2\sqrt{t}} + B_0 + B_1\frac{\sqrt{t}-\sqrt{t_0-t}}{\sqrt{t}+\sqrt{t_0-t}}\right),$$

where $k = \sqrt{t/4 - M_\pi^2}$ and $\sqrt{t_0} = 1.05\,\text{GeV}$, $B_0 = 1.043 \pm 0.011$, $B_1 = 0.19 \pm 0.05$ and $M_\rho = 773.6 \pm 0.9$ MeV [Garcia-Martin, Kaminski, Pelaez, Ruiz de Elvira, Ynduráin 2011]

- Correction for isospin breaking due to $\rho - \omega$ interference:

$$\begin{aligned} F_{\rho-\omega}(t) &= \left(1 + \epsilon\,\frac{t}{t_\omega - t}\right), \;\; t_\omega = (M_\omega - i/2\Gamma_\omega)^2, \\ \Delta\delta(t) &= \text{Arg}[F_{\rho-\omega}(t)] \end{aligned}$$

where, $M_\omega = 0.7826\text{GeV}$, $\Gamma_\omega = 0.0085\text{GeV}$ [Leutwyler 2002, Hanhart 2012]

- above t_{in} a continuous function for $\delta(t)$ is used that approaches asymptotically π [Abbas, Ananthanarayan, Caprini, Imsong, Ramanan 2010]

Phase Inputs

- phase is determined from Roy equation [Ananthanarayan, Colangelo, Gasser, Leutwyler 2001, Colangelo, Gasser, Leutwyler 2001, Kaminski, Pelaez, Ynduraín 2008, Garcia-Martin, Kaminski, Pelaez, Ruiz de Elvira, Ynduraín 2011]
- below $\sqrt{t_{\rm in}} = 0.917\text{GeV}$ the phase $\delta_1^1(t)$ is parametrized as,

$$\cot\delta_1^1(t) = \frac{\sqrt{t}}{2k^3}(M_\rho^2 - t)\left(\frac{2M_\pi^3}{M_\rho^2\sqrt{t}} + B_0 + B_1\frac{\sqrt{t}-\sqrt{t_0-t}}{\sqrt{t}+\sqrt{t_0-t}}\right),$$

  where $k = \sqrt{t/4 - M_\pi^2}$ and $\sqrt{t_0} = 1.05\,\text{GeV}$, $B_0 = 1.043 \pm 0.011$, $B_1 = 0.19 \pm 0.05$ and $M_\rho = 773.6 \pm 0.9$ MeV [Garcia-Martin, Kaminski, Pelaez, Ruiz de Elvira, Ynduraín 2011]
- Correction for isospin breaking due to $\rho - \omega$ interference:

$$\begin{aligned} F_{\rho-\omega}(t) &= \left(1 + \epsilon\frac{t}{t_\omega - t}\right), \quad t_\omega = (M_\omega - i/2\Gamma_\omega)^2, \\ \Delta\delta(t) &= \mathrm{Arg}[F_{\rho-\omega}(t)] \end{aligned}$$

  where, $M_\omega = 0.7826\text{GeV}$, $\Gamma_\omega = 0.0085\text{GeV}$ [Leutwyler 2002, Hanhart 2012]
- above $t_{\rm in}$ a continuous function for $\delta(t)$ is used that approaches asymptotically π [Abbas, Ananthanarayan, Caprini, Imsong, Ramanan 2010]

- phase is determined from Roy equation [Ananthanarayan, Colangelo, Gasser, Leutwyler 2001, Colangelo, Gasser, Leutwyler 2001, Kaminski, Pelaez, Ynduráin 2008, Garcia-Martin, Kaminski, Pelaez, Ruiz de Elvira, Ynduráin 2011]
- below $\sqrt{t_{\rm in}} = 0.917\mathrm{GeV}$ the phase $\delta_1^1(t)$ is parametrized as,

$$\cot\delta_1^1(t) = \frac{\sqrt{t}}{2k^3}(M_\rho^2 - t)\left(\frac{2M_\pi^3}{M_\rho^2\sqrt{t}} + B_0 + B_1\frac{\sqrt{t}-\sqrt{t_0-t}}{\sqrt{t}+\sqrt{t_0-t}}\right),$$

where $k=\sqrt{t/4-M_\pi^2}$ and $\sqrt{t_0} = 1.05\,\mathrm{GeV}$, $B_0 = 1.043 \pm 0.011$, $B_1 = 0.19 \pm 0.05$ and $M_\rho = 773.6 \pm 0.9$ MeV [Garcia-Martin, Kaminski, Pelaez, Ruiz de Elvira, Ynduráin 2011]

- Correction for isospin breaking due to $\rho-\omega$ interference:

$$F_{\rho-\omega}(t) = \left(1+\epsilon\frac{t}{t_\omega - t}\right), \quad t_\omega = (M_\omega - i/2\Gamma_\omega)^2,$$
$$\Delta\delta(t) = \mathrm{Arg}[F_{\rho-\omega}(t)]$$

where, $M_\omega = 0.7826\mathrm{GeV}$, $\Gamma_\omega = 0.0085\mathrm{GeV}$ [Leutwyler 2002, Hanhart 2012]

- above $t_{\rm in}$ a continuous function for $\delta(t)$ is used that approaches asymptotically π [Abbas, Ananthanarayan, Caprini, Imsong, Ramanan 2010]

Phase Inputs

- phase is determined from Roy equation [Ananthanarayan, Colangelo, Gasser, Leutwyler 2001, Colangelo, Gasser, Leutwyler 2001, Kaminski, Pelaez, Ynduráin 2008, Garcia-Martin, Kaminski, Pelaez, Ruiz de Elvira, Ynduráin 2011]
- below $\sqrt{t_{\rm in}} = 0.917\mathrm{GeV}$ the phase $\delta_1^1(t)$ is parametrized as,

$$\cot\delta_1^1(t) = \frac{\sqrt{t}}{2k^3}(M_\rho^2 - t)\left(\frac{2M_\pi^3}{M_\rho^2\sqrt{t}} + B_0 + B_1\frac{\sqrt{t}-\sqrt{t_0-t}}{\sqrt{t}+\sqrt{t_0-t}}\right),$$

  where $k = \sqrt{t/4 - M_\pi^2}$ and $\sqrt{t_0} = 1.05\,\mathrm{GeV}$, $B_0 = 1.043 \pm 0.011$, $B_1 = 0.19 \pm 0.05$ and $M_\rho = 773.6 \pm 0.9$ MeV [Garcia-Martin, Kaminski, Pelaez, Ruiz de Elvira, Ynduráin 2011]
- Correction for isospin breaking due to $\rho - \omega$ interference:

$$\begin{aligned} F_{\rho-\omega}(t) &= \left(1 + \epsilon\,\frac{t}{t_\omega - t}\right), \quad t_\omega = (M_\omega - i/2\Gamma_\omega)^2, \\ \Delta\delta(t) &= \mathrm{Arg}[F_{\rho-\omega}(t)] \end{aligned}$$

  where, $M_\omega = 0.7826\mathrm{GeV}$, $\Gamma_\omega = 0.0085\mathrm{GeV}$ [Leutwyler 2002, Hanhart 2012]
- above $t_{\rm in}$ a continuous function for $\delta(t)$ is used that approaches asymptotically π [Abbas, Ananthanarayan, Caprini, Imsong, Ramanan 2010]

Phase Inputs

- phase is determined from Roy equation [Ananthanarayan, Colangelo, Gasser, Leutwyler 2001, Colangelo, Gasser, Leutwyler 2001, Kaminski, Pelaez, Yndurain 2008, Garcia-Martin, Kaminski, Pelaez, Ruiz de Elvira, Yndurain 2011]
- below $\sqrt{t_{\rm in}} = 0.917\mathrm{GeV}$ the phase $\delta_1^1(t)$ is parametrized as,

$$\cot\delta_1^1(t) = \frac{\sqrt{t}}{2k^3}(M_\rho^2 - t)\left(\frac{2M_\pi^3}{M_\rho^2\sqrt{t}} + B_0 + B_1\frac{\sqrt{t}-\sqrt{t_0-t}}{\sqrt{t}+\sqrt{t_0-t}}\right),$$

  where $k = \sqrt{t/4 - M_\pi^2}$ and $\sqrt{t_0} = 1.05\,\mathrm{GeV}$, $B_0 = 1.043 \pm 0.011$, $B_1 = 0.19 \pm 0.05$ and $M_\rho = 773.6 \pm 0.9$ MeV [Garcia-Martin, Kaminski, Pelaez, Ruiz de Elvira, Yndurain 2011]
- Correction for isospin breaking due to $\rho - \omega$ interference:

$$\begin{aligned} F_{\rho-\omega}(t) &= \left(1 + \epsilon\,\frac{t}{t_\omega - t}\right), \quad t_\omega = (M_\omega - i/2\Gamma_\omega)^2, \\ \Delta\delta(t) &= \mathrm{Arg}[F_{\rho-\omega}(t)] \end{aligned}$$

  where, $M_\omega = 0.7826\mathrm{GeV}$, $\Gamma_\omega = 0.0085\mathrm{GeV}$ [Leutwyler 2002, Hanhart 2012]
- above $t_{\rm in}$ a continuous function for $\delta(t)$ is used that approaches asymptotically π [Abbas, Ananthanarayan, Caprini, Imsong, Ramanan 2010]

Weights used and Evaluations

- the value of I in Eq-(1) is calculated from $t_{\rm in}$ to $\sqrt{t} = 3\rm GeV$ using Babar data [Aubert et al (BABAR Collaboration). Phys. Rev. Lett. 103, 231801 (2009)]
- $3\,\rm GeV \leq \sqrt{t} \leq 20\rm GeV$ a constant modulus is chosen that is smoothly connected with a $1/t$ decrease above 20 GeV. [Ananthanarayan, Caprini, Imsong 2012]
- optimal bound is obtained with the following choices of $\rho(t)$ [Ananthanarayan, Caprini, Das, Imsong 2012]

$$\rho(t) = \frac{1}{t}, \quad \rho(t) = \frac{\sqrt{t}}{t+3}$$

β	γ	Q^2	I
0	1	0	0.578 ± 0.022
1/2	1	3	0.246 ± 0.011

- adopted range of charge radius [Colangelo 2004, Masjuan et al. 2008]

$$\langle r_\pi^2 \rangle = 0.43 \pm 0.01\,\text{fm}^2,$$

- spacelike inputs [Horn et al. 2006, Huber et al. 2008]

$$F(-1.60\,\rm GeV^2) = 0.243 \pm 0.012^{+0.019}_{-0.008}\,,$$

$$F(-2.45\,\rm GeV^2) = 0.167 \pm 0.010^{+0.013}_{-0.007}\,,$$

Weights used and Evaluations

- the value of I in Eq-(1) is calculated from t_{in} to $\sqrt{t} = 3\text{GeV}$ using Babar data [Aubert et al (BABAR Collaboration). Phys. Rev. Lett. 103, 231801 (2009)]
- $3\,\text{GeV} \leq \sqrt{t} \leq 20\text{GeV}$ a constant modulus is chosen that is smoothly connected with a $1/t$ decrease above 20 GeV. [Ananthanarayan, Caprini, Imsong 2012]
- optimal bound is obtained with the following choices of $\rho(t)$ [Ananthanarayan, Caprini, Das, Imsong 2012]

$$\rho(t) = \frac{1}{t}, \quad \rho(t) = \frac{\sqrt{t}}{t+3}$$

β	γ	Q^2	I
0	1	0	0.578 ± 0.022
1/2	1	3	0.246 ± 0.011

- adopted range of charge radius [Colangelo 2004, Masjuan et al. 2008]

$$\langle r_\pi^2 \rangle = 0.43 \pm 0.01\,\text{fm}^2,$$

- spacelike inputs [Horn et al. 2006, Huber et al. 2008]

$$F(-1.60\,\text{GeV}^2) = 0.243 \pm 0.012^{+0.019}_{-0.008}\,,$$

$$F(-2.45\,\text{GeV}^2) = 0.167 \pm 0.010^{+0.013}_{-0.007}\,,$$

- the value of I in Eq-(1) is calculated from $t_{\rm in}$ to $\sqrt{t} = 3\mathrm{GeV}$ using Babar data [Aubert et al (BABAR Collaboration). Phys. Rev. Lett. 103, 231801 (2009)]
- $3\,\mathrm{GeV} \leq \sqrt{t} \leq 20\mathrm{GeV}$ a constant modulus is chosen that is smoothly connected with a $1/t$ decrease above 20 GeV. [Ananthanarayan, Caprini, Imsong 2012]
- optimal bound is obtained with the following choices of $\rho(t)$ [Ananthanarayan, Caprini, Das, Imsong 2012]

$$\rho(t) = \frac{1}{t}, \quad \rho(t) = \frac{\sqrt{t}}{t+3}$$

β	γ	Q^2	I
0	1	0	0.578 ± 0.022
1/2	1	3	0.246 ± 0.011

- adopted range of charge radius [Colangelo 2004, Masjuan et al. 2008]

$$\langle r_\pi^2 \rangle = 0.43 \pm 0.01\,\mathrm{fm}^2,$$

- spacelike inputs [Horn et al. 2006, Huber et al. 2008]

$$F(-1.60\,\mathrm{GeV}^2) = 0.243 \pm 0.012^{+0.019}_{-0.008},$$

$$F(-2.45\,\mathrm{GeV}^2) = 0.167 \pm 0.010^{+0.013}_{-0.007},$$

Weights used and Evaluations

- the value of I in Eq-(1) is calculated from $t_{\rm in}$ to $\sqrt{t} = 3\text{GeV}$ using Babar data [Aubert et al (BABAR Collaboration). Phys. Rev. Lett. 103, 231801 (2009)]
- $3\,\text{GeV} \leq \sqrt{t} \leq 20\text{GeV}$ a constant modulus is chosen that is smoothly connected with a $1/t$ decrease above 20 GeV. [Ananthanarayan, Caprini, Imsong 2012]
- optimal bound is obtained with the following choices of $\rho(t)$ [Ananthanarayan, Caprini, Das, Imsong 2012]

$$\rho(t) = \frac{1}{t}, \quad \rho(t) = \frac{\sqrt{t}}{t+3}$$

β	γ	Q^2	I
0	1	0	0.578 ± 0.022
1/2	1	3	0.246 ± 0.011

- adopted range of charge radius [Colangelo 2004, Masjuan et al. 2008]

$$\langle r_\pi^2 \rangle = 0.43 \pm 0.01\,\text{fm}^2,$$

- spacelike inputs [Horn et al. 2006, Huber et al. 2008]

$$F(-1.60\,\text{GeV}^2) = 0.243 \pm 0.012^{+0.019}_{-0.008}\,,$$
$$F(-2.45\,\text{GeV}^2) = 0.167 \pm 0.010^{+0.013}_{-0.007}\,,$$

Weights used and Evaluations

- the value of I in Eq-(1) is calculated from $t_{\rm in}$ to $\sqrt{t} = 3\text{GeV}$ using Babar data [Aubert et al (BABAR Collaboration). Phys. Rev. Lett. 103, 231801 (2009)]
- $3\,\text{GeV} \leq \sqrt{t} \leq 20\text{GeV}$ a constant modulus is chosen that is smoothly connected with a $1/t$ decrease above 20 GeV. [Ananthanarayan, Caprini, Imsong 2012]
- optimal bound is obtained with the following choices of $\rho(t)$ [Ananthanarayan, Caprini, Das, Imsong 2012]

$$\rho(t) = \frac{1}{t}, \quad \rho(t) = \frac{\sqrt{t}}{t+3}$$

β	γ	Q^2	I
0	1	0	0.578 ± 0.022
1/2	1	3	0.246 ± 0.011

- adopted range of charge radius [Colangelo 2004, Masjuan et al. 2008]

$$\langle r_\pi^2 \rangle = 0.43 \pm 0.01\,\text{fm}^2,$$

- spacelike inputs [Horn et al. 2006, Huber et al. 2008]

$$F(-1.60\,\text{GeV}^2) = 0.243 \pm 0.012^{+0.019}_{-0.008}\,,$$

$$F(-2.45\,\text{GeV}^2) = 0.167 \pm 0.010^{+0.013}_{-0.007}\,,$$

Weights used and Evaluations

- the value of I in Eq-(1) is calculated from $t_{\rm in}$ to $\sqrt{t} = 3{\rm GeV}$ using Babar data [Aubert et al (BABAR Collaboration). Phys. Rev. Lett. 103, 231801 (2009)]
- $3\,{\rm GeV} \leq \sqrt{t} \leq 20{\rm GeV}$ a constant modulus is chosen that is smoothly connected with a $1/t$ decrease above 20 GeV. [Ananthanarayan, Caprini, Imsong 2012]
- optimal bound is obtained with the following choices of $\rho(t)$ [Ananthanarayan, Caprini, Das, Imsong 2012]

$$\rho(t) = \frac{1}{t}, \quad \rho(t) = \frac{\sqrt{t}}{t+3}$$

β	γ	Q^2	I
0	1	0	0.578 ± 0.022
1/2	1	3	0.246 ± 0.011

- adopted range of charge radius [Colangelo 2004, Masjuan et al. 2008]

$$\langle r_\pi^2 \rangle = 0.43 \pm 0.01\,\text{fm}^2,$$

- spacelike inputs [Horn et al. 2006, Huber et al. 2008]

$$F(-1.60\,{\rm GeV}^2) = 0.243 \pm 0.012^{+0.019}_{-0.008}\,,$$
$$F(-2.45\,{\rm GeV}^2) = 0.167 \pm 0.010^{+0.013}_{-0.007}\,,$$

Recent High Statistics Experiments

BABAR [Phys. Rev. Lett. **103**, 231801 ,Phys. Rev. D **86**, 032013]

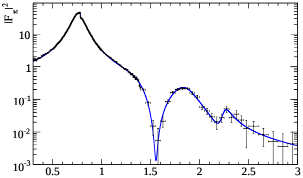

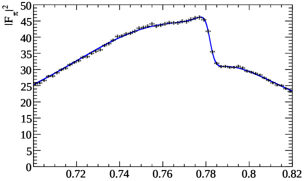

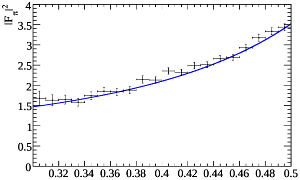

The pion form factor-squared measured by BABAR from 0.3 GeV to 3 GeV. The VDM fit is shown in blue.

- BABAR detector at SLAC PEP-II asymmetric energy e^+e^- storage ring operated at $\Upsilon(4S)$ resonance
- 2012 analysis is based on 232 fb^{-1} of data

BABAR [Phys. Rev. Lett. **103**, 231801 ,Phys. Rev. D **86**, 032013]

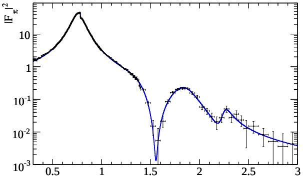

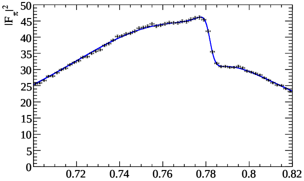

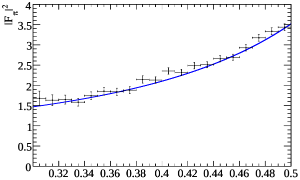

The pion form factor-squared measured by BABAR from 0.3 GeV to 3 GeV. The VDM fit is shown in blue.

- BABAR detector at SLAC PEP-II asymmetric energy e^+e^- storage ring operated at $\Upsilon(4S)$ resonance
- 2012 analysis is based on 232 fb^{-1} of data

BABAR [Phys. Rev. Lett. **103**, 231801 ,Phys. Rev. D **86**, 032013]

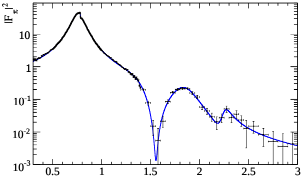

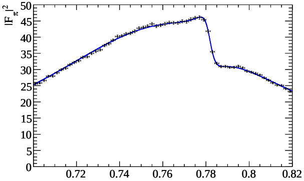

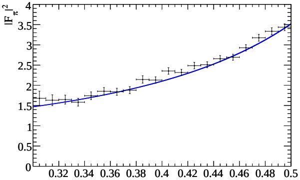

The pion form factor-squared measured by BABAR from 0.3 GeV to 3 GeV. The VDM fit is shown in blue.

- BABAR detector at SLAC PEP-II asymmetric energy e^+e^- storage ring operated at $\Upsilon(4S)$ resonance
- 2012 analysis is based on 232 fb^{-1} of data

BABAR

BABAR [Phys. Rev. Lett. **103**, 231801 ,Phys. Rev. D **86**, 032013]

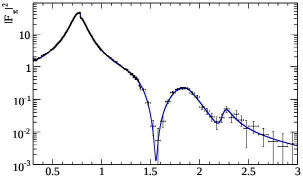

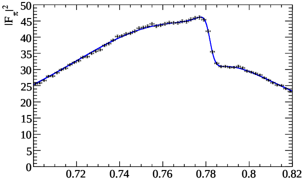

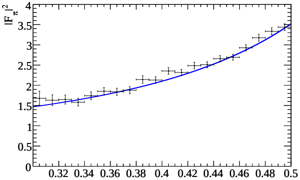

The pion form factor-squared measured by BABAR from 0.3 GeV to 3 GeV. The VDM fit is shown in blue.

- BABAR detector at SLAC PEP-II asymmetric energy e^+e^- storage ring operated at $\Upsilon(4S)$ resonance
- 2012 analysis is based on 232 fb^{-1} of data

SND and CMD-2

SND is a VEPP-2M e^+e^- detector operated between 1995 to 2000. It measured $|F_\pi|^2$ from cross section determination in the region $\sqrt{s} < 1000\mathrm{MeV}$ [J.Exp.Theor.Phys. 103 (2006) 38].

CMD-2 [Phys.Lett. B578 (2004) 285-289 , JETP Lett. 84 (2006) 413-417, Phys.Lett. B648 (2007) 28-38]

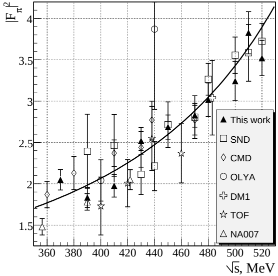

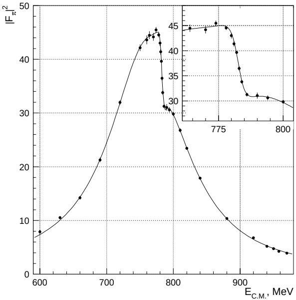

- CMD-2 is also a VEPP-2M e^+e^- detector in Novosibirsk, Russia.
- analysis is based on 56 nb^{-1} of data

SND and CMD-2

SND is a VEPP-2M e^+e^- detector operated between 1995 to 2000. It measured $|F_\pi|^2$ from cross section determination in the region $\sqrt{s} < 1000\mathrm{MeV}$ [J.Exp.Theor.Phys. 103 (2006) 38].

CMD-2 [Phys.Lett. B578 (2004) 285-289 , JETP Lett. 84 (2006) 413-417, Phys.Lett. B648 (2007) 28-38]

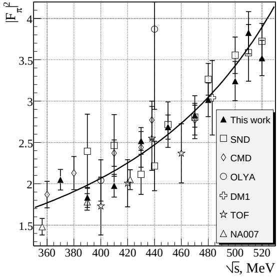

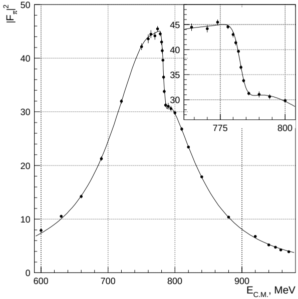

- CMD-2 is also a VEPP-2M e^+e^- detector in Novosibirsk, Russia.
- analysis is based on 56 nb^{-1} of data

SND and CMD-2

SND is a VEPP-2M e^+e^- detector operated between 1995 to 2000. It measured $|F_\pi|^2$ from cross section determination in the region $\sqrt{s} < 1000\text{MeV}$ [J.Exp.Theor.Phys. 103 (2006) 38].

CMD-2 [Phys.Lett. B578 (2004) 285-289 , JETP Lett. 84 (2006) 413-417, Phys.Lett. B648 (2007) 28-38]

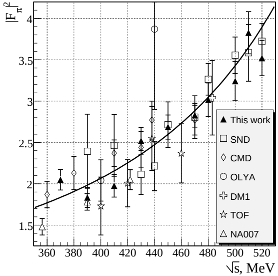

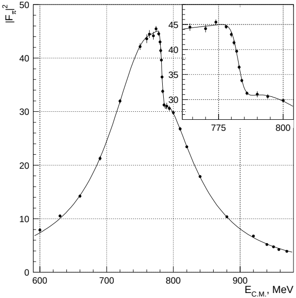

- CMD-2 is also a VEPP-2M e^+e^- detector in Novosibirsk, Russia.
- analysis is based on 56 nb^{-1} of data

SND is a VEPP-2M e^+e^- detector operated between 1995 to 2000. It measured $|F_\pi|^2$ from cross section determination in the region $\sqrt{s} < 1000\mathrm{MeV}$ [J.Exp.Theor.Phys. 103 (2006) 38].
CMD-2 [Phys.Lett. B578 (2004) 285-289 , JETP Lett. 84 (2006) 413-417, Phys.Lett. B648 (2007) 28-38]

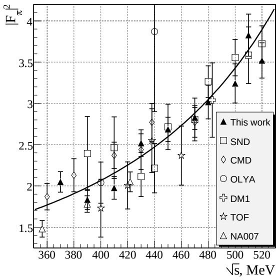

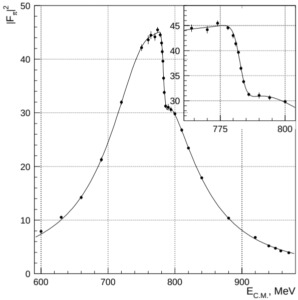

- CMD-2 is also a VEPP-2M e^+e^- detector in Novosibirsk, Russia.
- analysis is based on 56 nb^{-1} of data

SND is a VEPP-2M e^+e^- detector operated between 1995 to 2000. It measured $|F_\pi|^2$ from cross section determination in the region $\sqrt{s} < 1000\mathrm{MeV}$ [J.Exp.Theor.Phys. 103 (2006) 38].
CMD-2 [Phys.Lett. B578 (2004) 285-289 , JETP Lett. 84 (2006) 413-417, Phys.Lett. B648 (2007) 28-38]

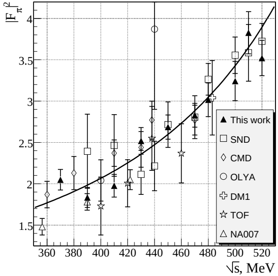

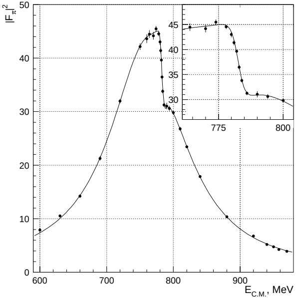

- CMD-2 is also a VEPP-2M e^+e^- detector in Novosibirsk, Russia.
- analysis is based on 56 nb^{-1} of data

KLOE

KLOE [Phys.Lett. B670 (2009) 285, Phys.Lett. B700 (2011) 102, Phys.Lett. B720 (2013) 336]

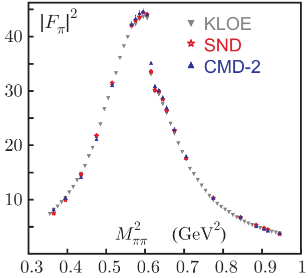

- The KLOE detector is at DAΦNE, the Frascati ϕ-factory
- e^+e^- collider running at center of mass energy equal to the ϕ meson mass
- the analysis is based on 2.5 fb^{-1} of data

KLOE [Phys.Lett. B670 (2009) 285, Phys.Lett. B700 (2011) 102, Phys.Lett. B720 (2013) 336]

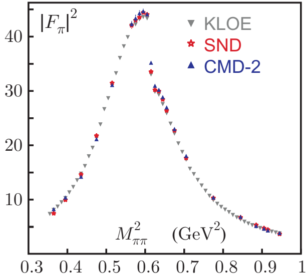

- The KLOE detector is at DAΦNE, the Frascati ϕ-factory
- e^+e^- collider running at center of mass energy equal to the ϕ meson mass
- the analysis is based on 2.5 fb^{-1} of data

KLOE [Phys.Lett. B670 (2009) 285, Phys.Lett. B700 (2011) 102, Phys.Lett. B720 (2013) 336]

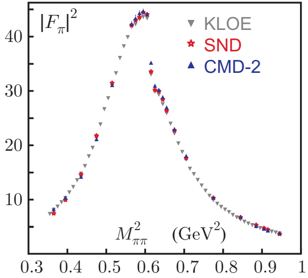

- The KLOE detector is at DAΦNE, the Frascati ϕ-factory
- e^+e^- collider running at center of mass energy equal to the ϕ meson mass
- the analysis is based on 2.5 fb^{-1} of data

KLOE [Phys.Lett. B670 (2009) 285, Phys.Lett. B700 (2011) 102, Phys.Lett. B720 (2013) 336]

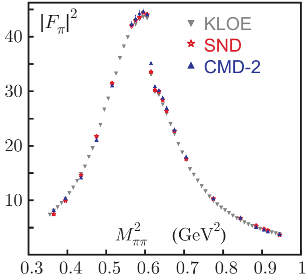

- The KLOE detector is at DAΦNE, the Frascati ϕ-factory
- e^+e^- collider running at center of mass energy equal to the ϕ meson mass
- the analysis is based on 2.5 fb^{-1} of data

KLOE [Phys.Lett. B670 (2009) 285, Phys.Lett. B700 (2011) 102, Phys.Lett. B720 (2013) 336]

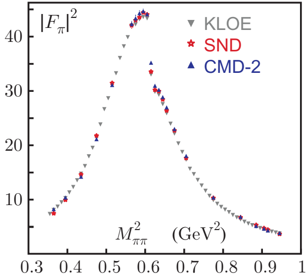

- The KLOE detector is at DAΦNE, the Frascati ϕ-factory
- e^+e^- collider running at center of mass energy equal to the ϕ meson mass
- the analysis is based on 2.5 fb^{-1} of data

KLOE [Phys.Lett. B670 (2009) 285, Phys.Lett. B700 (2011) 102, Phys.Lett. B720 (2013) 336]

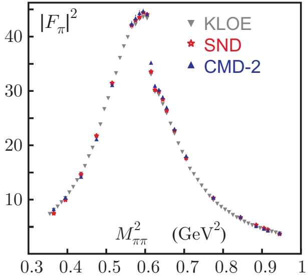

- The KLOE detector is at DAΦNE, the Frascati ϕ-factory
- e^+e^- collider running at center of mass energy equal to the ϕ meson mass
- the analysis is based on 2.5 fb^{-1} of data

Bounds on modulus

Results: bounds on modulus

- Spacelike inputs: obtained from Jefferson Laboratory experiment

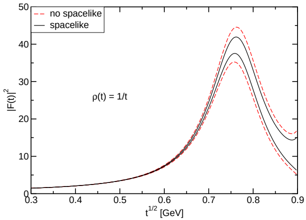

$F(-1.60\,\mathrm{GeV}^2)$ for upper bound and $F(-2.45\,\mathrm{GeV}^2)$ for lower bound [Ananthanarayan, Caprini, Das, Imsong 2012]

Results: bounds on modulus

- Spacelike inputs: obtained from Jefferson Laboratory experiment

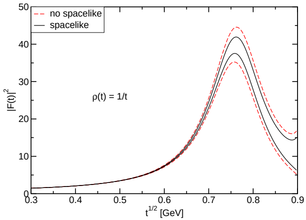

$F(-1.60\,\mathrm{GeV}^2)$ for upper bound and $F(-2.45\,\mathrm{GeV}^2)$ for lower bound [Ananthanarayan, Caprini, Das, Imsong 2012]

Results: bounds on modulus

inclusion of uncertainties of inputs

- Method 1: each input separately varied, with the others kept fixed at their central values
- Method 2: all the inputs are simultaneously varied within their allowed interval and the conservative bound is taken–largest upper bound and smallest lower bound

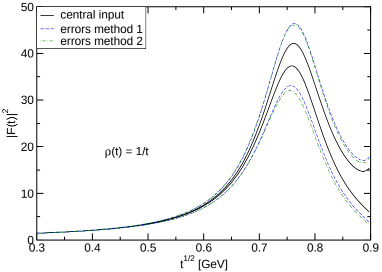

inclusion of uncertainties of inputs

- Method 1: each input separately varied, with the others kept fixed at their central values
- Method 2: all the inputs are simultaneously varied within their allowed interval and the conservative bound is taken–largest upper bound and smallest lower bound

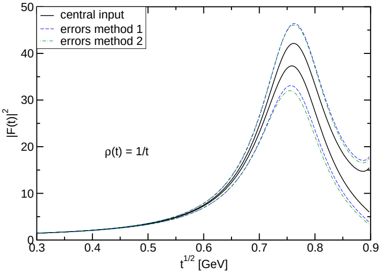

Results: bounds on modulus

inclusion of uncertainties of inputs

- Method 1: each input separately varied, with the others kept fixed at their central values
- Method 2: all the inputs are simultaneously varied within their allowed interval and the conservative bound is taken–largest upper bound and smallest lower bound

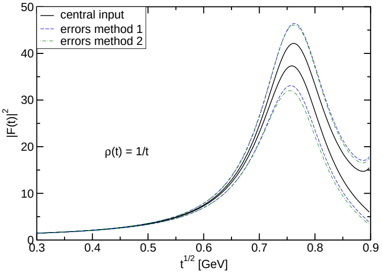

Results: bounds on modulus

inclusion of uncertainties of inputs

- Method 1: each input separately varied, with the others kept fixed at their central values
- Method 2: all the inputs are simultaneously varied within their allowed interval and the conservative bound is taken–largest upper bound and smallest lower bound

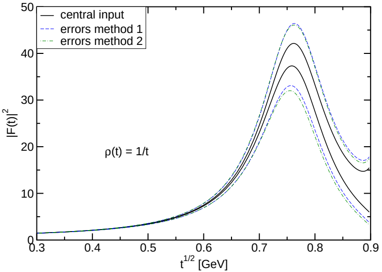

Bounds without isospin correction due to $\rho - \omega$ interference [Ananthanarayan, Caprini, Das, Imsong 2012]

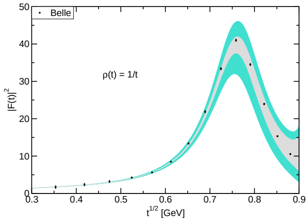

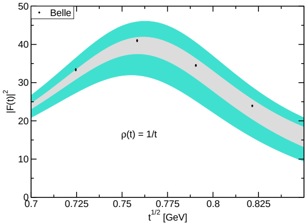

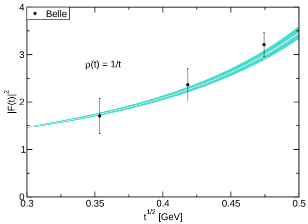

- above the ρ peak, data are consistent with central band
- below ρ peak data are at the upper edge of the central band

Results: bounds on modulus

Bounds without isospin correction due to $\rho - \omega$ interference [Ananthanarayan, Caprini, Das, Imsong 2012]

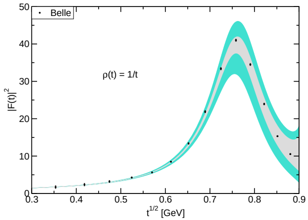

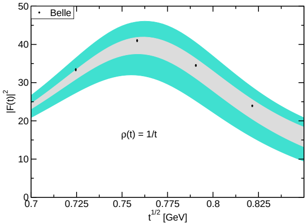

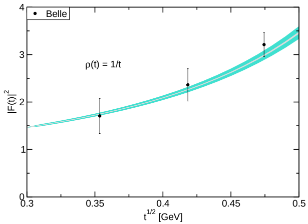

- above the ρ peak, data are consistent with central band
- below ρ peak data are at the upper edge of the central band

Bounds without isospin correction due to $\rho - \omega$ interference [Ananthanarayan, Caprini, Das, Imsong 2012]

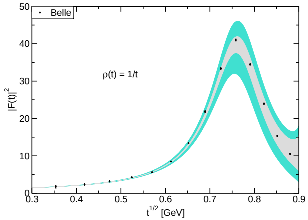

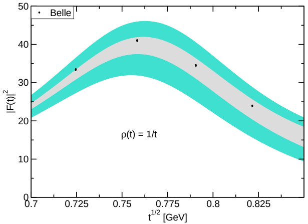

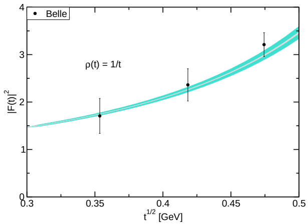

- above the ρ peak, data are consistent with central band
- below ρ peak data are at the upper edge of the central band

Bounds without isospin correction due to $\rho - \omega$ interference [Ananthanarayan, Caprini, Das, Imsong 2012]

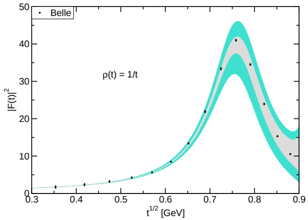

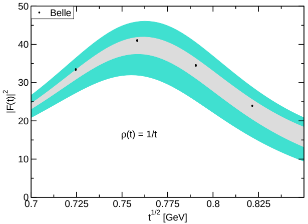

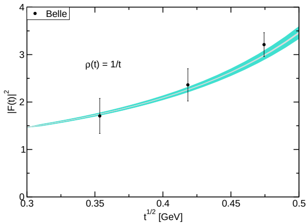

- above the ρ peak, data are consistent with central band
- below ρ peak data are at the upper edge of the central band

Bounds without isospin correction due to $\rho - \omega$ interference [Ananthanarayan, Caprini, Das, Imsong 2012]

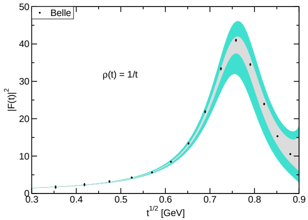

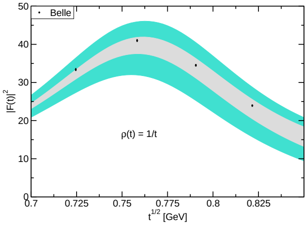

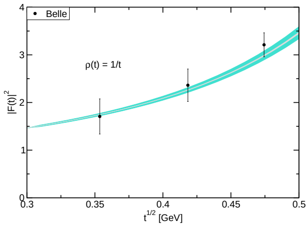

- above the ρ peak, data are consistent with central band
- below ρ peak data are at the upper edge of the central band

Results: bounds on modulus

Bounds with isospin correction correction due to $\rho - \omega$ interference [Ananthanarayan, Caprini, Das, Imsong 2012]

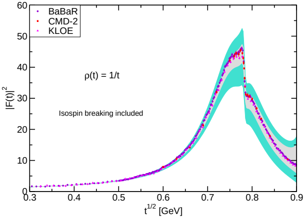

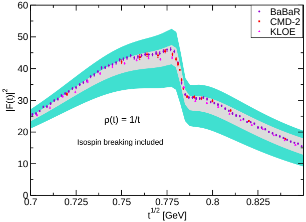

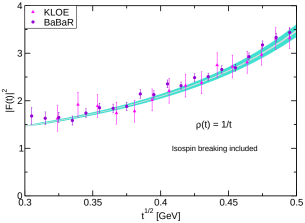

- above the ρ peak, data are consistent with central band
- below ρ peak data are at the upper edge of the central band

Results: bounds on modulus

Bounds with isospin correction correction due to $\rho - \omega$ interference [Ananthanarayan, Caprini, Das, Imsong 2012]

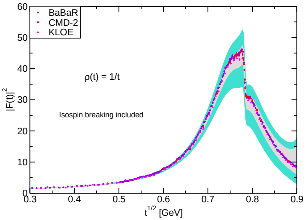

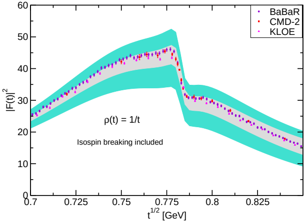

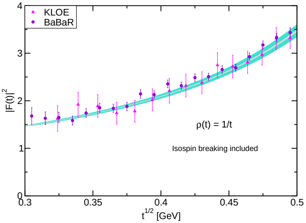

- above the ρ peak, data are consistent with central band
- below ρ peak data are at the upper edge of the central band

Bounds with isospin correction correction due to $\rho - \omega$ interference [Ananthanarayan, Caprini, Das, Imsong 2012]

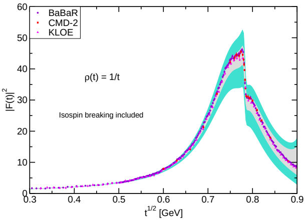

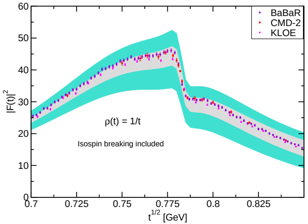

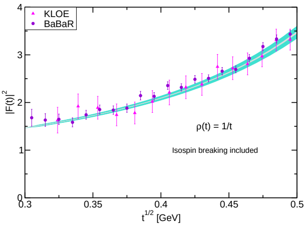

- above the ρ peak, data are consistent with central band
- below ρ peak data are at the upper edge of the central band

Results: bounds on modulus

Bounds with isospin correction correction due to $\rho - \omega$ interference [Ananthanarayan, Caprini, Das, Imsong 2012]

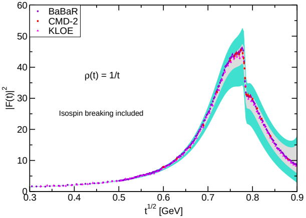

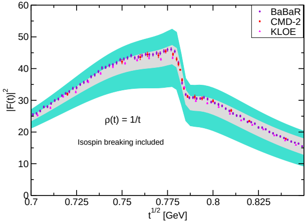

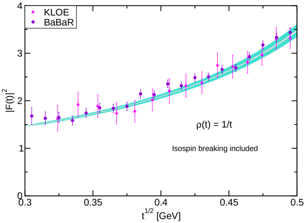

- above the ρ peak, data are consistent with central band
- below ρ peak data are at the upper edge of the central band

Optimization of inputs [Ananthanarayan, Caprini, Das, Imsong 2012]

Sensitivity to charge radius

- $\langle r_\pi^2 \rangle = 0.435\,\mathrm{fm}^2$ shifts the bound upwards below ρ peak
- $\langle r_\pi^2 \rangle = 0.435\,\mathrm{fm}^2$ the bound is above data
- full consistency by varying charge radius is not possible

Sensitivity to phase

- tests with the central value increased/decreased by quoted error
- higher phase leads to bound shifted upwards
- bounds are sensitive to overall shape of the phase, rather than magnitude

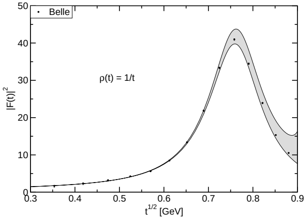

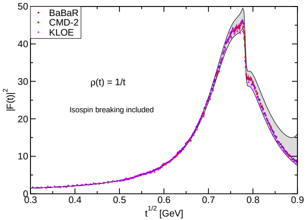

Results: bounds on modulus

Optimization of inputs [Ananthanarayan, Caprini, Das, Imsong 2012]

Sensitivity to charge radius

- $\langle r_\pi^2 \rangle = 0.435\,\mathrm{fm}^2$ shifts the bound upwards below ρ peak
- $\langle r_\pi^2 \rangle = 0.435\,\mathrm{fm}^2$ the bound is above data
- full consistency by varying charge radius is not possible

Sensitivity to phase

- tests with the central value increased/decreased by quoted error
- higher phase leads to bound shifted upwards
- bounds are sensitive to overall shape of the phase, rather than magnitude

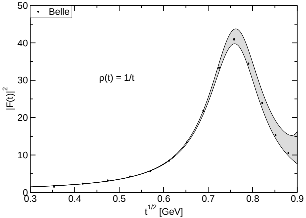

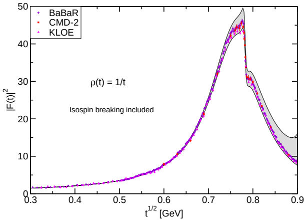

Results: bounds on modulus

Optimization of inputs [Ananthanarayan, Caprini, Das, Imsong 2012]

Sensitivity to charge radius

- $\langle r_\pi^2 \rangle = 0.435\,\mathrm{fm}^2$ shifts the bound upwards below ρ peak
- $\langle r_\pi^2 \rangle = 0.435\,\mathrm{fm}^2$ the bound is above data
- full consistency by varying charge radius is not possible

Sensitivity to phase

- tests with the central value increased/decreased by quoted error
- higher phase leads to bound shifted upwards
- bounds are sensitive to overall shape of the phase, rather than magnitude

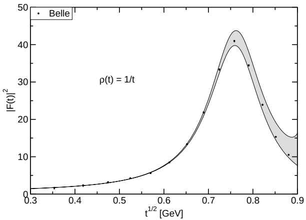

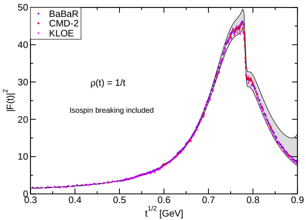

Results: bounds on modulus

Optimization of inputs [Ananthanarayan, Caprini, Das, Imsong 2012]

Sensitivity to charge radius

- $\langle r_\pi^2 \rangle = 0.435\,\text{fm}^2$ shifts the bound upwards below ρ peak
- $\langle r_\pi^2 \rangle = 0.435\,\text{fm}^2$ the bound is above data
- full consistency by varying charge radius is not possible

Sensitivity to phase

- tests with the central value increased/decreased by quoted error
- higher phase leads to bound shifted upwards
- bounds are sensitive to overall shape of the phase, rather than magnitude

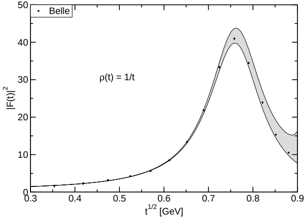

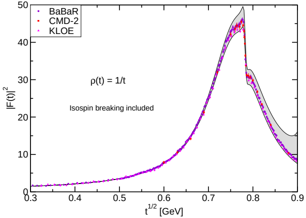

Results: bounds on modulus

Optimization of inputs [Ananthanarayan, Caprini, Das, Imsong 2012]

Sensitivity to charge radius

- $\langle r_\pi^2 \rangle = 0.435\,\mathrm{fm}^2$ shifts the bound upwards below ρ peak
- $\langle r_\pi^2 \rangle = 0.435\,\mathrm{fm}^2$ the bound is above data
- full consistency by varying charge radius is not possible

Sensitivity to phase

- tests with the central value increased/decreased by quoted error
- higher phase leads to bound shifted upwards
- bounds are sensitive to overall shape of the phase, rather than magnitude

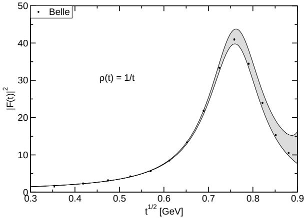

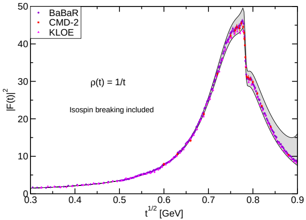

Optimization of inputs [Ananthanarayan, Caprini, Das, Imsong 2012]

Sensitivity to charge radius

- $\langle r_\pi^2 \rangle = 0.435\,\text{fm}^2$ shifts the bound upwards below ρ peak
- $\langle r_\pi^2 \rangle = 0.435\,\text{fm}^2$ the bound is above data
- full consistency by varying charge radius is not possible

Sensitivity to phase

- tests with the central value increased/decreased by quoted error
- higher phase leads to bound shifted upwards
- bounds are sensitive to overall shape of the phase, rather than magnitude

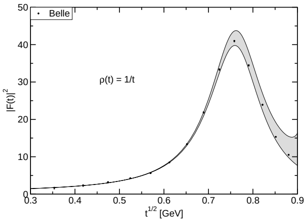

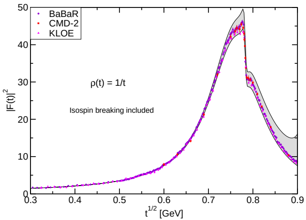

Results: bounds on modulus

Optimization of inputs [Ananthanarayan, Caprini, Das, Imsong 2012]

Sensitivity to charge radius

- $\langle r_\pi^2 \rangle = 0.435\,\mathrm{fm}^2$ shifts the bound upwards below ρ peak
- $\langle r_\pi^2 \rangle = 0.435\,\mathrm{fm}^2$ the bound is above data
- full consistency by varying charge radius is not possible

Sensitivity to phase

- tests with the central value increased/decreased by quoted error
- higher phase leads to bound shifted upwards
- bounds are sensitive to overall shape of the phase, rather than magnitude

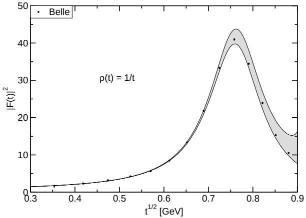

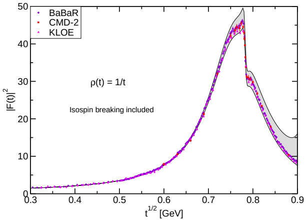

Results: bounds on modulus

Optimization of inputs [Ananthanarayan, Caprini, Das, Imsong 2012]

Sensitivity to charge radius

- $\langle r_\pi^2 \rangle = 0.435\,\text{fm}^2$ shifts the bound upwards below ρ peak
- $\langle r_\pi^2 \rangle = 0.435\,\text{fm}^2$ the bound is above data
- full consistency by varying charge radius is not possible

Sensitivity to phase

- tests with the central value increased/decreased by quoted error
- higher phase leads to bound shifted upwards
- bounds are sensitive to overall shape of the phase, rather than magnitude

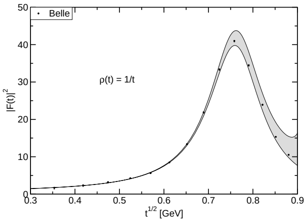

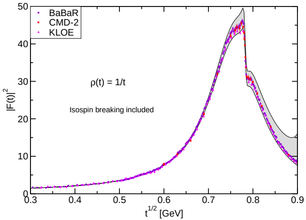

Optimization of inputs [Ananthanarayan, Caprini, Das, Imsong 2012]

Sensitivity to charge radius

- $\langle r_\pi^2 \rangle = 0.435\,\text{fm}^2$ shifts the bound upwards below ρ peak
- $\langle r_\pi^2 \rangle = 0.435\,\text{fm}^2$ the bound is above data
- full consistency by varying charge radius is not possible

Sensitivity to phase

- tests with the central value increased/decreased by quoted error
- higher phase leads to bound shifted upwards
- bounds are sensitive to overall shape of the phase, rather than magnitude

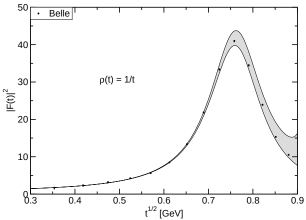

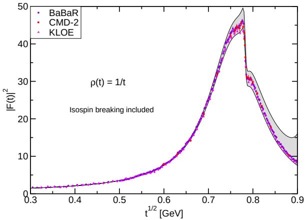

Results: bounds on modulus

Optimization of inputs [Ananthanarayan, Caprini, Das, Imsong 2012]

Sensitivity to charge radius

- $\langle r_\pi^2 \rangle = 0.435\,\mathrm{fm}^2$ shifts the bound upwards below ρ peak
- $\langle r_\pi^2 \rangle = 0.435\,\mathrm{fm}^2$ the bound is above data
- full consistency by varying charge radius is not possible

Sensitivity to phase

- tests with the central value increased/decreased by quoted error
- higher phase leads to bound shifted upwards
- bounds are sensitive to overall shape of the phase, rather than magnitude

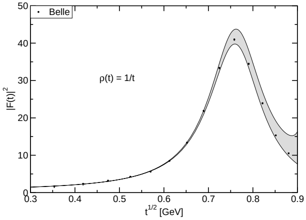

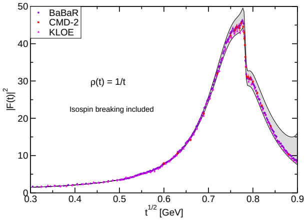

Results: bounds on modulus

Optimal bounds
[Ananthanarayan, Caprini, Das, Imsong 2012]

choices of weight functions $\rho(t)$

- $\rho(t) = 1/t$ leads to better upper bound and $\rho(t) = t^{1/2}/(t+3)$ leads to better lower bound

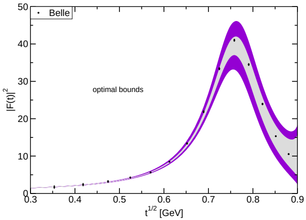

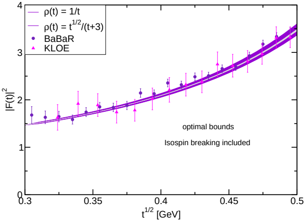

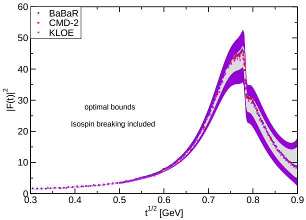

Optimal bounds
[Ananthanarayan, Caprini, Das, Imsong 2012]

choices of weight functions $\rho(t)$

- $\rho(t) = 1/t$ leads to better upper bound and $\rho(t) = t^{1/2}/(t+3)$ leads to better lower bound

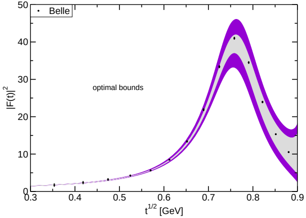

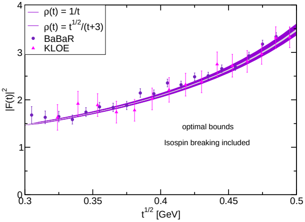

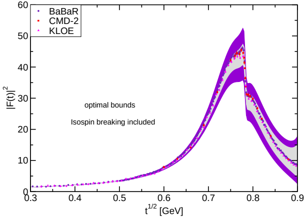

Results: bounds on modulus

Optimal bounds
[Ananthanarayan, Caprini, Das, Imsong 2012]

choices of weight functions $\rho(t)$

- $\rho(t) = 1/t$ leads to better upper bound and $\rho(t) = t^{1/2}/(t+3)$ leads to better lower bound

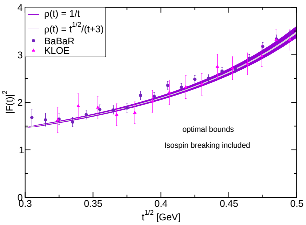

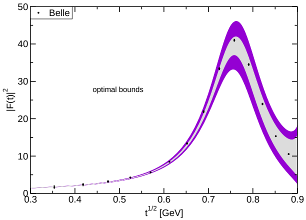

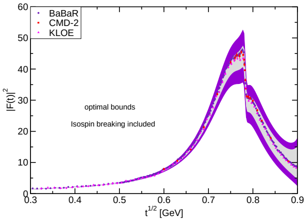

Rigorous properties of the bounds

The following observations may be made for the bounds we derive. That they

- Are optimal for a given input
- Are independent of the phase $\delta(t)$ of the Omnès function for $t > t_{in}$
- For a fixed weight $\rho(t)$, they depend in a monotonous way on I, becoming stronger/weaker when this value is decreased/increased

Rigorous properties of the bounds

The following observations may be made for the bounds we derive. That they

- Are optimal for a given input
- Are independent of the phase $\delta(t)$ of the Omnès function for $t > t_{in}$
- For a fixed weight $\rho(t)$, they depend in a monotonous way on I, becoming stronger/weaker when this value is decreased/increased

Rigorous properties of the bounds

The following observations may be made for the bounds we derive. That they

- Are optimal for a given input
- Are independent of the phase $\delta(t)$ of the Omnès function for $t > t_{in}$
- For a fixed weight $\rho(t)$, they depend in a monotonous way on I, becoming stronger/weaker when this value is decreased/increased

Rigorous properties of the bounds

The following observations may be made for the bounds we derive. That they

- Are optimal for a given input
- Are independent of the phase $\delta(t)$ of the Omnès function for $t > t_{in}$
- For a fixed weight $\rho(t)$, they depend in a monotonous way on I, becoming stronger/weaker when this value is decreased/increased

Rigorous properties of the bounds

The following observations may be made for the bounds we derive. That they

- Are optimal for a given input
- Are independent of the phase $\delta(t)$ of the Omnès function for $t > t_{in}$
- For a fixed weight $\rho(t)$, they depend in a monotonous way on I, becoming stronger/weaker when this value is decreased/increased

Conclusions: bounds on modulus

- overall no inconsistency
- at low energy our bound are stringent
- knowledge of form factor below 0.5 Gev can be improved
- slight inconsistency between our bound and Babar data at low energies

Conclusions: bounds on modulus

- overall no inconsistency
- at low energy our bound are stringent
- knowledge of form factor below 0.5 Gev can be improved
- slight inconsistency between our bound and Babar data at low energies

Conclusions: bounds on modulus

- overall no inconsistency
- at low energy our bound are stringent
- knowledge of form factor below 0.5 Gev can be improved
- slight inconsistency between our bound and Babar data at low energies

Conclusions: bounds on modulus

- overall no inconsistency
- at low energy our bound are stringent
- knowledge of form factor below 0.5 Gev can be improved
- slight inconsistency between our bound and Babar data at low energies

Conclusions: bounds on modulus

- overall no inconsistency
- at low energy our bound are stringent
- knowledge of form factor below 0.5 Gev can be improved
- slight inconsistency between our bound and Babar data at low energies

Precision bounds on shape parameters

[Ananthanarayan, Caprini, Das, Imsong 2012]

- drastic variation at low energies
- at low energies, for several experimental points no solution to $\langle r_\pi^2 \rangle$ is found
- final allowed range is the intersection of the allowed ranges at fixed energies
- intersection is empty when all points are considered: inconsistencies in data between measurements at different energies

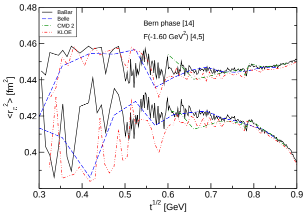

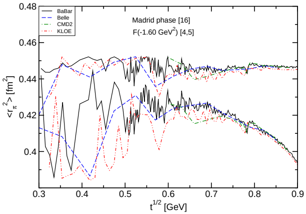

[Ananthanarayan, Caprini, Das, Imsong 2012]

- drastic variation at low energies
- at low energies, for several experimental points no solution to $\langle r_\pi^2 \rangle$ is found
- final allowed range is the intersection of the allowed ranges at fixed energies
- intersection is empty when all points are considered: inconsistencies in data between measurements at different energies

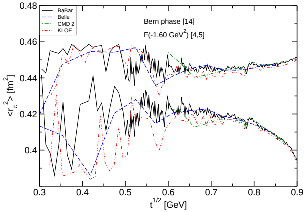

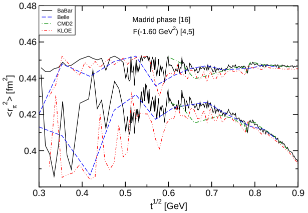

[Ananthanarayan, Caprini, Das, Imsong 2012]

- drastic variation at low energies
- at low energies, for several experimental points no solution to $\langle r_\pi^2 \rangle$ is found
- final allowed range is the intersection of the allowed ranges at fixed energies
- intersection is empty when all points are considered: inconsistencies in data between measurements at different energies

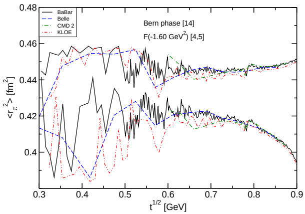

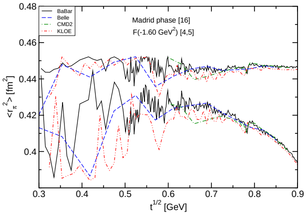

[Ananthanarayan, Caprini, Das, Imsong 2012]

- drastic variation at low energies
- at low energies, for several experimental points no solution to $\langle r_\pi^2 \rangle$ is found
- final allowed range is the intersection of the allowed ranges at fixed energies
- intersection is empty when all points are considered: inconsistencies in data between measurements at different energies

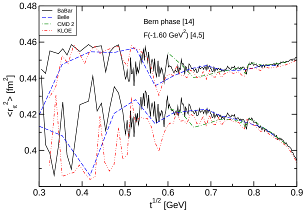

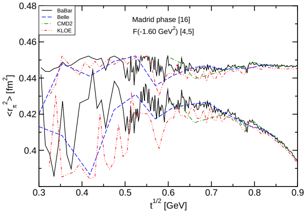

[Ananthanarayan, Caprini, Das, Imsong 2012]

- drastic variation at low energies
- at low energies, for several experimental points no solution to $\langle r_\pi^2 \rangle$ is found
- final allowed range is the intersection of the allowed ranges at fixed energies
- intersection is empty when all points are considered: inconsistencies in data between measurements at different energies

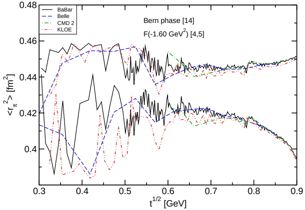

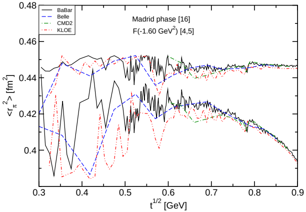

[Ananthanarayan, Caprini, Das, Imsong 2012]

- drastic variation at low energies
- at low energies, for several experimental points no solution to $\langle r_\pi^2 \rangle$ is found
- final allowed range is the intersection of the allowed ranges at fixed energies
- intersection is empty when all points are considered: inconsistencies in data between measurements at different energies

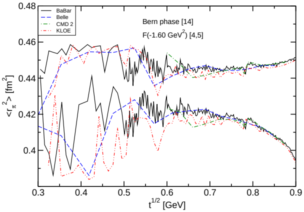

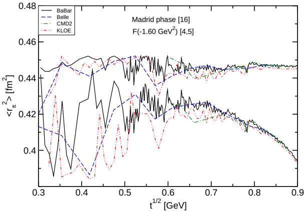

[Ananthanarayan, Caprini, Das, Imsong 2012]

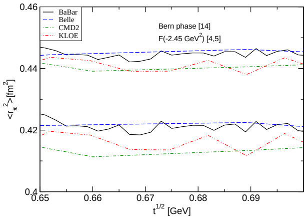

- for prediction, we restrict ourselves from 0.65 GeV to 0.70 GeV ("stability region")
- strict intersection leads to

$$\langle r_\pi^2 \rangle_{\min} \approx 0.42\,\mathrm{fm}^2, \quad \langle r_\pi^2 \rangle_{\max} \approx 0.44\,\mathrm{fm}^2.$$

- weighted average leads to

$$\langle r_\pi^2 \rangle_{\min,\,\mathrm{av}} \approx 0.40\,\mathrm{fm}^2, \quad \langle r_\pi^2 \rangle_{\max,\,\mathrm{av}} \approx 0.45\,\mathrm{fm}^2$$

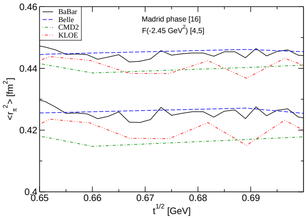

[Ananthanarayan, Caprini, Das, Imsong 2012]

- for prediction, we restrict ourselves from 0.65 GeV to 0.70 GeV ("stability region")
- strict intersection leads to

$$\langle r_\pi^2 \rangle_{\min} \approx 0.42\,\mathrm{fm}^2, \quad \langle r_\pi^2 \rangle_{\max} \approx 0.44\,\mathrm{fm}^2.$$

- weighted average leads to

$$\langle r_\pi^2 \rangle_{\min,\,\mathrm{av}} \approx 0.40\,\mathrm{fm}^2, \quad \langle r_\pi^2 \rangle_{\max,\,\mathrm{av}} \approx 0.45\,\mathrm{fm}^2$$

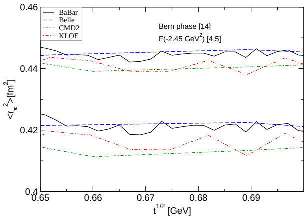

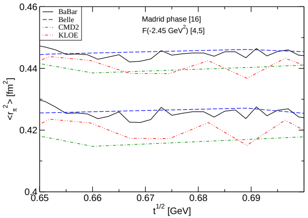

[Ananthanarayan, Caprini, Das, Imsong 2012]

- for prediction, we restrict ourselves from 0.65 GeV to 0.70 GeV (“stability region”)
- strict intersection leads to

$$\langle r_\pi^2 \rangle_{\rm min} \approx 0.42\,{\rm fm}^2, \quad \langle r_\pi^2 \rangle_{\rm max} \approx 0.44\,{\rm fm}^2.$$

- weighted average leads to

$$\langle r_\pi^2 \rangle_{\rm min,\,av} \approx 0.40\,{\rm fm}^2, \quad \langle r_\pi^2 \rangle_{\rm max,\,av} \approx 0.45\,{\rm fm}^2$$

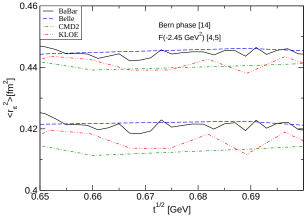

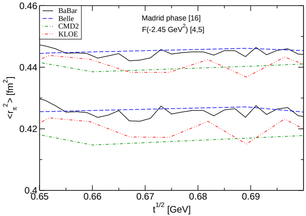

[Ananthanarayan, Caprini, Das, Imsong 2012]

- for prediction, we restrict ourselves from 0.65 GeV to 0.70 GeV (“stability region”)
- strict intersection leads to

$$\langle r_\pi^2 \rangle_{\mathrm{min}} \approx 0.42\,\mathrm{fm}^2, \quad \langle r_\pi^2 \rangle_{\mathrm{max}} \approx 0.44\,\mathrm{fm}^2.$$

- weighted average leads to

$$\langle r_\pi^2 \rangle_{\mathrm{min,\,av}} \approx 0.40\,\mathrm{fm}^2, \quad \langle r_\pi^2 \rangle_{\mathrm{max,\,av}} \approx 0.45\,\mathrm{fm}^2$$

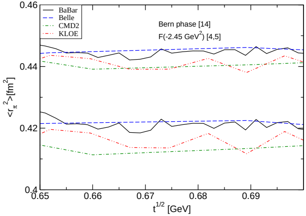

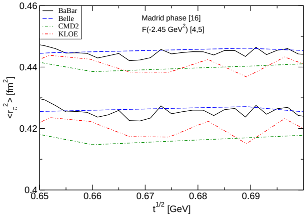

[Ananthanarayan, Caprini, Das, Imsong 2012]

- for prediction, we restrict ourselves from 0.65 GeV to 0.70 GeV ("stability region")
- strict intersection leads to

$$\langle r_\pi^2 \rangle_{\min} \approx 0.42\,\mathrm{fm}^2, \quad \langle r_\pi^2 \rangle_{\max} \approx 0.44\,\mathrm{fm}^2.$$

- weighted average leads to

$$\langle r_\pi^2 \rangle_{\min,\,\mathrm{av}} \approx 0.40\,\mathrm{fm}^2, \quad \langle r_\pi^2 \rangle_{\max,\,\mathrm{av}} \approx 0.45\,\mathrm{fm}^2$$

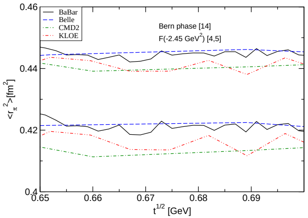

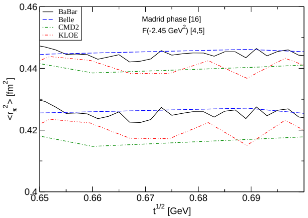

[Ananthanarayan, Caprini, Das, Imsong 2012]

$$c \in \ (3.79,\ 4.00)\ \mathrm{GeV}^{-4},$$
$$d \in \ (10.14,\ 10.56)\ \mathrm{GeV}^{-6},$$

- higher shape parameters are sensitive to modulus data
- the bounds shown are for timelike modulus data from Babar
- should be regarded as provisional
- a previous analysis with $\langle r_\pi^2 \rangle = 0.435 \pm 0.005$

$$c \in \ (3.75,\ 3.98)\ \mathrm{GeV}^{-4},$$
$$d \in \ (9.91,\ 10.45)\ \mathrm{GeV}^{-6},$$

[Ananthanarayan, Caprini, Imsong 2011]

- $c = 3.9\mathrm{GeV}^{-4}$ and $d = 9.70\mathrm{GeV}^{-6}$ [Truong 1998]

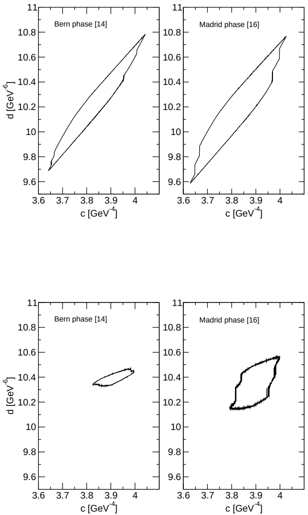

$c - d$

[Ananthanarayan, Caprini, Das, Imsong 2012]

$$c \in (3.79,\, 4.00)\ \mathrm{GeV}^{-4},$$
$$d \in (10.14,\, 10.56)\ \mathrm{GeV}^{-6},$$

- higher shape parameters are sensitive to modulus data
- the bounds shown are for timelike modulus data from Babar
- should be regarded as provisional
- a previous analysis with $\langle r_\pi^2 \rangle = 0.435 \pm 0.005$

$$c \in (3.75,\, 3.98)\ \mathrm{GeV}^{-4},$$
$$d \in (9.91,\, 10.45)\ \mathrm{GeV}^{-6},$$

[Ananthanarayan, Caprini, Imsong 2011]

- $c = 3.9\mathrm{GeV}^{-4}$ and $d = 9.70\mathrm{GeV}^{-6}$ [Truong 1998]

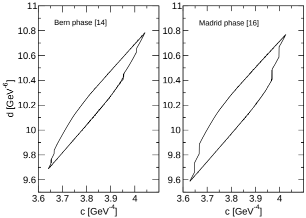

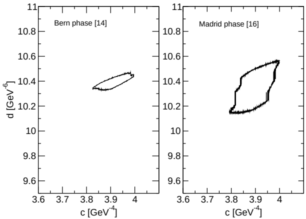

$c-d$

[Ananthanarayan, Caprini, Das, Imsong 2012]

$$c \in \ (3.79,\ 4.00)\,\mathrm{GeV}^{-4},$$
$$d \in \ (10.14,\ 10.56)\,\mathrm{GeV}^{-6},$$

- higher shape parameters are sensitive to modulus data
- the bounds shown are for timelike modulus data from Babar
- should be regarded as provisional
- a previous analysis with $\langle r_\pi^2 \rangle = 0.435 \pm 0.005$

$$c \in \ (3.75,\ 3.98)\,\mathrm{GeV}^{-4},$$
$$d \in \ (9.91,\ 10.45)\,\mathrm{GeV}^{-6},$$

  [Ananthanarayan, Caprini, Imsong 2011]
- $c = 3.9\mathrm{GeV}^{-4}$ and $d = 9.70\mathrm{GeV}^{-6}$ [Truong 1998]

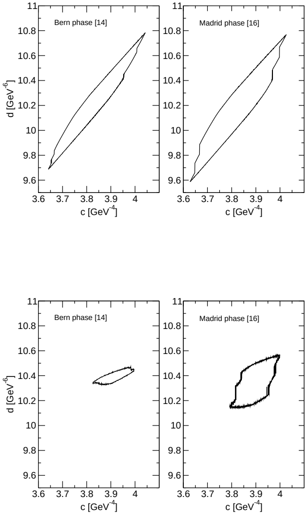

$c - d$

[Ananthanarayan, Caprini, Das, Imsong 2012]

$$c \in \ (3.79,\ 4.00)\,\mathrm{GeV}^{-4},$$
$$d \in \ (10.14,\ 10.56)\,\mathrm{GeV}^{-6},$$

- higher shape parameters are sensitive to modulus data
- the bounds shown are for timelike modulus data from Babar
- should be regarded as provisional
- a previous analysis with $\langle r_\pi^2 \rangle = 0.435 \pm 0.005$

$$c \in \ (3.75,\ 3.98)\,\mathrm{GeV}^{-4},$$
$$d \in \ (9.91,\ 10.45)\,\mathrm{GeV}^{-6},$$

  [Ananthanarayan, Caprini, Imsong 2011]
- $c = 3.9\mathrm{GeV}^{-4}$ and $d = 9.70\mathrm{GeV}^{-6}$ [Truong 1998]

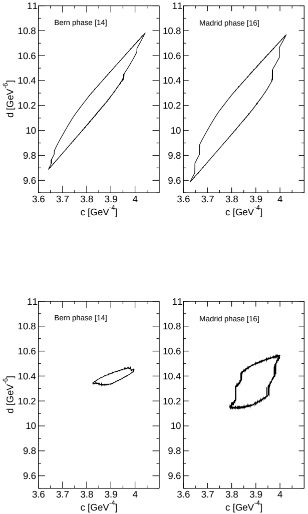

[Ananthanarayan, Caprini, Das, Imsong 2012]

$$c \in \ (3.79,\ 4.00)\,\mathrm{GeV}^{-4},$$
$$d \in \ (10.14,\ 10.56)\,\mathrm{GeV}^{-6},$$

- higher shape parameters are sensitive to modulus data
- the bounds shown are for timelike modulus data from Babar
- should be regarded as provisional
- a previous analysis with $\langle r_\pi^2 \rangle = 0.435 \pm 0.005$

$$c \in \ (3.75,\ 3.98)\,\mathrm{GeV}^{-4},$$
$$d \in \ (9.91,\ 10.45)\,\mathrm{GeV}^{-6},$$

[Ananthanarayan, Caprini, Imsong 2011]

- $c = 3.9\mathrm{GeV}^{-4}$ and $d = 9.70\mathrm{GeV}^{-6}$ [Truong 1998]

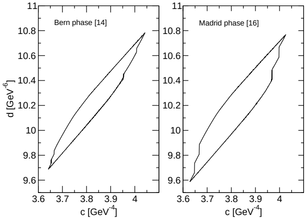

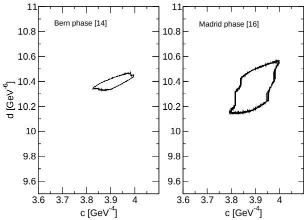

[Ananthanarayan, Caprini, Das, Imsong 2012]

$$c \in \ (3.79,\ 4.00)\,\mathrm{GeV}^{-4},$$
$$d \in \ (10.14,\ 10.56)\,\mathrm{GeV}^{-6},$$

- higher shape parameters are sensitive to modulus data
- the bounds shown are for timelike modulus data from Babar
- should be regarded as provisional
- a previous analysis with $\langle r_\pi^2 \rangle = 0.435 \pm 0.005$

$$c \in \ (3.75,\ 3.98)\,\mathrm{GeV}^{-4},$$
$$d \in \ (9.91,\ 10.45)\,\mathrm{GeV}^{-6},$$

[Ananthanarayan, Caprini, Imsong 2011]
- $c = 3.9\mathrm{GeV}^{-4}$ and $d = 9.70\mathrm{GeV}^{-6}$ [Truong 1998]

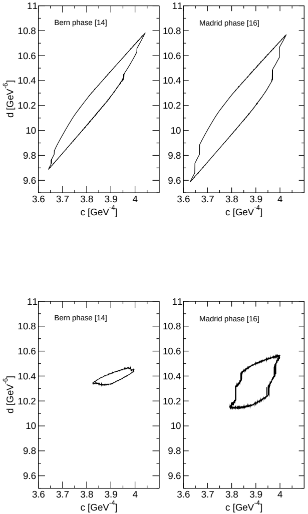

$c - d$

[Ananthanarayan, Caprini, Das, Imsong 2012]

$$c \in \ (3.79,\ 4.00)\,\mathrm{GeV}^{-4},$$
$$d \in \ (10.14,\ 10.56)\,\mathrm{GeV}^{-6},$$

- higher shape parameters are sensitive to modulus data
- the bounds shown are for timelike modulus data from Babar
- should be regarded as provisional
- a previous analysis with $\langle r_\pi^2 \rangle = 0.435 \pm 0.005$

$$c \in \ (3.75,\ 3.98)\,\mathrm{GeV}^{-4},$$
$$d \in \ (9.91,\ 10.45)\,\mathrm{GeV}^{-6},$$

  [Ananthanarayan, Caprini, Imsong 2011]
- $c = 3.9\mathrm{GeV}^{-4}$ and $d = 9.70\mathrm{GeV}^{-6}$ [Truong 1998]

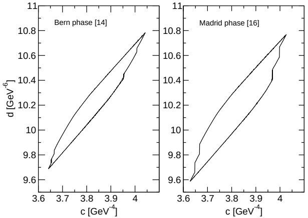

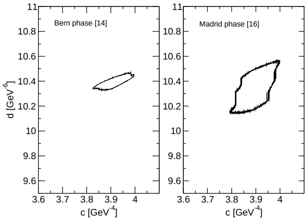

$c - d$

[Ananthanarayan, Caprini, Das, Imsong 2012]

$$c \in \ (3.79,\ 4.00)\ \mathrm{GeV}^{-4},$$
$$d \in \ (10.14,\ 10.56)\ \mathrm{GeV}^{-6},$$

- higher shape parameters are sensitive to modulus data
- the bounds shown are for timelike modulus data from Babar
- should be regarded as provisional
- a previous analysis with $\langle r_\pi^2 \rangle = 0.435 \pm 0.005$

$$c \in \ (3.75,\ 3.98)\ \mathrm{GeV}^{-4},$$
$$d \in \ (9.91,\ 10.45)\ \mathrm{GeV}^{-6},$$

  [Ananthanarayan, Caprini, Imsong 2011]

- $c = 3.9 \mathrm{GeV}^{-4}$ and $d = 9.70 \mathrm{GeV}^{-6}$ [Truong 1998]

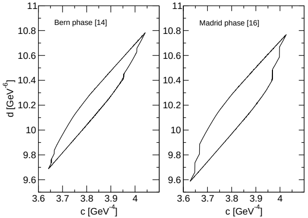

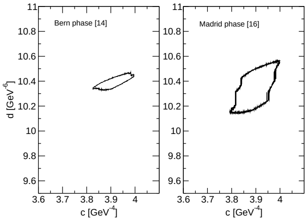

Conclusions: bounds on shape parameters

- lower and upper limit on charge radius

$$\langle r_\pi^2 \rangle \in (0.42, 0.44)\,\mathrm{fm}^2$$

- higher shape parameters are sensitive to timelike modulus data
- and yet we have quite stringent predictions that have narrowed down the allowed range to a few percent
- bounds on higher shape parameters require precise data

Conclusions: bounds on shape parameters

- lower and upper limit on charge radius

$$\langle r_\pi^2 \rangle \in (0.42, 0.44)\,\mathrm{fm}^2$$

- higher shape parameters are sensitive to timelike modulus data
- and yet we have quite stringent predictions that have narrowed down the allowed range to a few percent
- bounds on higher shape parameters require precise data

Conclusions: bounds on shape parameters

- lower and upper limit on charge radius

$$\langle r_\pi^2 \rangle \in (0.42, 0.44)\,\mathrm{fm}^2$$

- higher shape parameters are sensitive to timelike modulus data
- and yet we have quite stringent predictions that have narrowed down the allowed range to a few percent
- bounds on higher shape parameters require precise data

Conclusions: bounds on shape parameters

- lower and upper limit on charge radius

$$\langle r_\pi^2 \rangle \in (0.42, 0.44)\,\mathrm{fm}^2$$

- higher shape parameters are sensitive to timelike modulus data
- and yet we have quite stringent predictions that have narrowed down the allowed range to a few percent
- bounds on higher shape parameters require precise data

Conclusions: bounds on shape parameters

- lower and upper limit on charge radius

$$\langle r_\pi^2 \rangle \in (0.42, 0.44)\,\mathrm{fm}^2$$

- higher shape parameters are sensitive to timelike modulus data
- and yet we have quite stringent predictions that have narrowed down the allowed range to a few percent
- bounds on higher shape parameters require precise data

Pionic contribution to the muon $(g-2)$ from e^+e^- experiments

Pionic contribution to muon $(g-2)$

- The present numbers for a_μ in the SM and the experimental value read:
  - $116591803(1)(42)(26) \times 10^{-11)}$ where the errors come from QED, had, etc
  - $11659209.1(5.4)(3.3) \times 10^{-10}$ where the errors are sys and stat.
- future experimental precision: $\delta_\mu^{expt} \sim 16 \times 10^{-11}$
- current theoretical precision: $\delta_\mu^{th} \sim 49 \times 10^{-11}$
- at low energy large theory uncertainty from non-perturbative hadronic contribution ($\delta_\mu^{LOVP} \sim 41 \times 10^{-11}$)
- large uncertainty in low energy experimental data on cross section

We determine two-pion contribution to muon $(g-2)$ based on our improved knowledge on the modulus of pion electromagnetic form factor at low energy. [Ananthanarayan, Caprini, Das, Imsong, arXiv:1312.5849]

Pionic contribution to muon $(g-2)$

- The present numbers for a_μ in the SM and the experimental value read:
  - $116591803(1)(42)(26) \times 10^{-11)}$ where the errors come from QED, had, etc
  - $11659209.1(5.4)(3.3) \times 10^{-10}$ where the errors are sys and stat.
- future experimental precision: $\delta_\mu^{expt} \sim 16 \times 10^{-11}$
- current theoretical precision: $\delta_\mu^{th} \sim 49 \times 10^{-11}$
- at low energy large theory uncertainty from non-perturbative hadronic contribution ($\delta_\mu^{LOVP} \sim 41 \times 10^{-11}$)
- large uncertainty in low energy experimental data on cross section

We determine two-pion contribution to muon $(g-2)$ based on our improved knowledge on the modulus of pion electromagnetic form factor at low energy. [Ananthanarayan, Caprini, Das, Imsong, arXiv:1312.5849]

Pionic contribution to muon $(g-2)$

- The present numbers for a_μ in the SM and the experimental value read:
  - $116591803(1)(42)(26) \times 10^{-11)}$ where the errors come from QED, had, etc
  - $11659209.1(5.4)(3.3) \times 10^{-10}$ where the errors are sys and stat.
- future experimental precision: $\delta_\mu^{expt} \sim 16 \times 10^{-11}$
- current theoretical precision: $\delta_\mu^{th} \sim 49 \times 10^{-11}$
- at low energy large theory uncertainty from non-perturbative hadronic contribution ($\delta_\mu^{LOVP} \sim 41 \times 10^{-11}$)
- large uncertainty in low energy experimental data on cross section

We determine two-pion contribution to muon $(g-2)$ based on our improved knowledge on the modulus of pion electromagnetic form factor at low energy. [Ananthanarayan, Caprini, Das, Imsong, arXiv:1312.5849]

- The present numbers for a_μ in the SM and the experimental value read:
  - $116591803(1)(42)(26) \times 10^{-11)}$ where the errors come from QED, had, etc
  - $11659209.1(5.4)(3.3) \times 10^{-10}$ where the errors are sys and stat.
- future experimental precision: $\delta_\mu^{expt} \sim 16 \times 10^{-11}$
- current theoretical precision: $\delta_\mu^{th} \sim 49 \times 10^{-11}$
- at low energy large theory uncertainty from non-perturbative hadronic contribution ($\delta_\mu^{LOVP} \sim 41 \times 10^{-11}$)
- large uncertainty in low energy experimental data on cross section

We determine two-pion contribution to muon $(g-2)$ based on our improved knowledge on the modulus of pion electromagnetic form factor at low energy. [Ananthanarayan, Caprini, Das, Imsong, arXiv:1312.5849]

Pionic contribution to muon $(g-2)$

- The present numbers for a_μ in the SM and the experimental value read:
  - $116591803(1)(42)(26) \times 10^{-11)}$ where the errors come from QED, had, etc
  - $11659209.1(5.4)(3.3) \times 10^{-10}$ where the errors are sys and stat.
- future experimental precision: $\delta_\mu^{expt} \sim 16 \times 10^{-11}$
- current theoretical precision: $\delta_\mu^{th} \sim 49 \times 10^{-11}$
- at low energy large theory uncertainty from non-perturbative hadronic contribution ($\delta_\mu^{LOVP} \sim 41 \times 10^{-11}$)
- large uncertainty in low energy experimental data on cross section

We determine two-pion contribution to muon $(g-2)$ based on our improved knowledge on the modulus of pion electromagnetic form factor at low energy. [Ananthanarayan, Caprini, Das, Imsong, arXiv:1312.5849]

Pionic contribution to muon $(g-2)$

- The present numbers for a_μ in the SM and the experimental value read:
  - $116591803(1)(42)(26) \times 10^{-11)}$ where the errors come from QED, had, etc
  - $11659209.1(5.4)(3.3) \times 10^{-10}$ where the errors are sys and stat.
- future experimental precision: $\delta_\mu^{expt} \sim 16 \times 10^{-11}$
- current theoretical precision: $\delta_\mu^{th} \sim 49 \times 10^{-11}$
- at low energy large theory uncertainty from non-perturbative hadronic contribution ($\delta_\mu^{LOVP} \sim 41 \times 10^{-11}$)
- large uncertainty in low energy experimental data on cross section

We determine two-pion contribution to muon $(g-2)$ based on our improved knowledge on the modulus of pion electromagnetic form factor at low energy. [Ananthanarayan, Caprini, Das, Imsong, arXiv:1312.5849]

Pionic contribution to muon $(g-2)$

- The present numbers for a_μ in the SM and the experimental value read:
  - $116591803(1)(42)(26) \times 10^{-11)}$ where the errors come from QED, had, etc
  - $11659209.1(5.4)(3.3) \times 10^{-10}$ where the errors are sys and stat.
- future experimental precision: $\delta_\mu^{expt} \sim 16 \times 10^{-11}$
- current theoretical precision: $\delta_\mu^{th} \sim 49 \times 10^{-11}$
- at low energy large theory uncertainty from non-perturbative hadronic contribution ($\delta_\mu^{LOVP} \sim 41 \times 10^{-11}$)
- large uncertainty in low energy experimental data on cross section

We determine two-pion contribution to muon $(g-2)$ based on our improved knowledge on the modulus of pion electromagnetic form factor at low energy. [Ananthanarayan, Caprini, Das, Imsong, arXiv:1312.5849]

Pionic contribution to muon $(g-2)$

- The present numbers for a_μ in the SM and the experimental value read:
  - $116591803(1)(42)(26) \times 10^{-11)}$ where the errors come from QED, had, etc
  - $11659209.1(5.4)(3.3) \times 10^{-10}$ where the errors are sys and stat.
- future experimental precision: $\delta_\mu^{expt} \sim 16 \times 10^{-11}$
- current theoretical precision: $\delta_\mu^{th} \sim 49 \times 10^{-11}$
- at low energy large theory uncertainty from non-perturbative hadronic contribution ($\delta_\mu^{LOVP} \sim 41 \times 10^{-11}$)
- large uncertainty in low energy experimental data on cross section

We determine two-pion contribution to muon $(g-2)$ based on our improved knowledge on the modulus of pion electromagnetic form factor at low energy. [Ananthanarayan, Caprini, Das, Imsong, arXiv:1312.5849]

Pionic contribution to muon $(g-2)$

- The present numbers for a_μ in the SM and the experimental value read:
  - $116591803(1)(42)(26) \times 10^{-11)}$ where the errors come from QED, had, etc
  - $11659209.1(5.4)(3.3) \times 10^{-10}$ where the errors are sys and stat.
- future experimental precision: $\delta_\mu^{expt} \sim 16 \times 10^{-11}$
- current theoretical precision: $\delta_\mu^{th} \sim 49 \times 10^{-11}$
- at low energy large theory uncertainty from non-perturbative hadronic contribution ($\delta_\mu^{LOVP} \sim 41 \times 10^{-11}$)
- large uncertainty in low energy experimental data on cross section

We determine two-pion contribution to muon $(g-2)$ based on our improved knowledge on the modulus of pion electromagnetic form factor at low energy. [Ananthanarayan, Caprini, Das, Imsong, arXiv:1312.5849]

Motivation

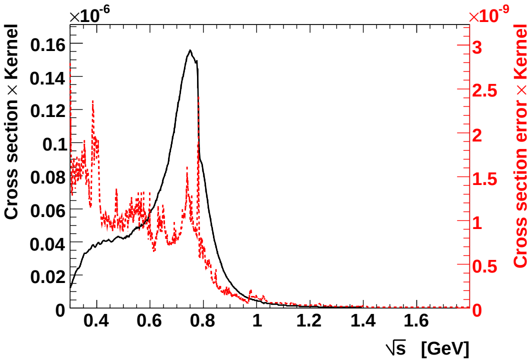

- Black: the cross section for the combined e^+e^- data multiplied by the kernel function $K(s)$ in the integral for a_μ
- Red: the corresponding error contribution, with statistical and systematic errors added in quadrature

[M. Davier, A. Hoecker, B. Malaescu, C.Z. Yuan and Z. Zhang, Eur.Phys.J. C66 (2010) 1, arXiv:0908.4300]

Motivation

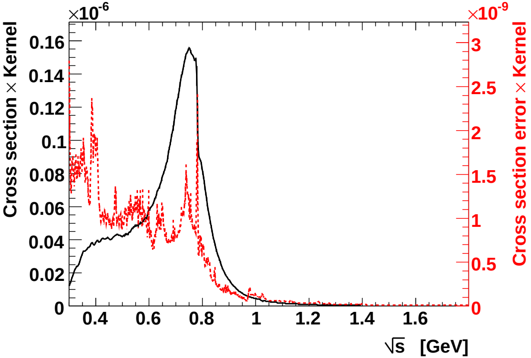

- Black: the cross section for the combined e^+e^- data multiplied by the kernel function $K(s)$ in the integral for a_μ
- Red: the corresponding error contribution, with statistical and systematic errors added in quadrature

[M. Davier, A. Hoecker, B. Malaescu, C.Z. Yuan and Z. Zhang, Eur.Phys.J. C66 (2010) 1, arXiv:0908.4300]

Motivation

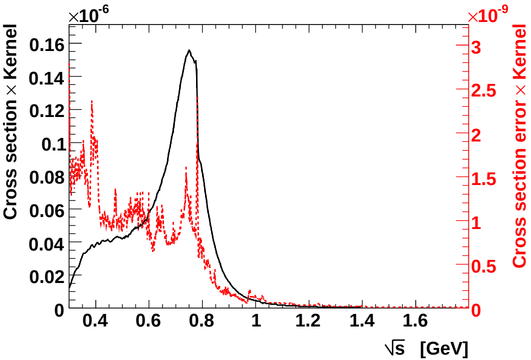

- Black: the cross section for the combined e^+e^- data multiplied by the kernel function $K(s)$ in the integral for a_μ
- Red: the corresponding error contribution, with statistical and systematic errors added in quadrature

[M. Davier, A. Hoecker, B. Malaescu, C.Z. Yuan and Z. Zhang, Eur.Phys.J. C66 (2010) 1, arXiv:0908.4300]

Motivation

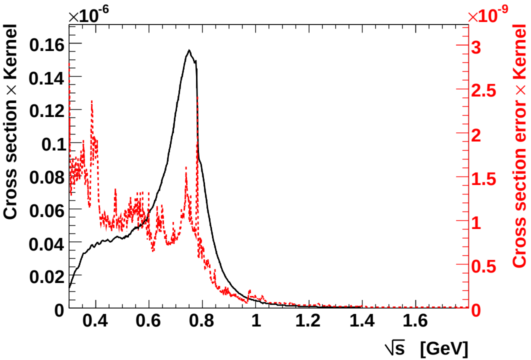

- Black: the cross section for the combined e^+e^- data multiplied by the kernel function $K(s)$ in the integral for a_μ
- Red: the corresponding error contribution, with statistical and systematic errors added in quadrature

[M. Davier, A. Hoecker, B. Malaescu, C.Z. Yuan and Z. Zhang, Eur.Phys.J. C66 (2010) 1, arXiv:0908.4300]

Motivation

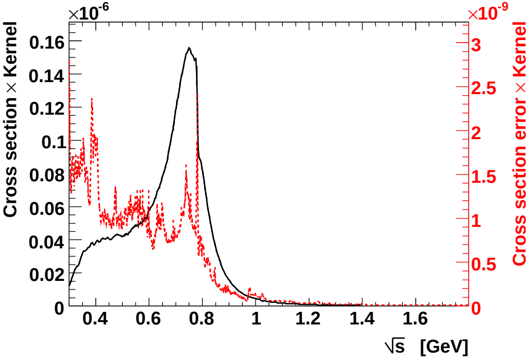

- Black: the cross section for the combined e^+e^- data multiplied by the kernel function $K(s)$ in the integral for a_μ
- Red: the corresponding error contribution, with statistical and systematic errors added in quadrature

[M. Davier, A. Hoecker, B. Malaescu, C.Z. Yuan and Z. Zhang, Eur.Phys.J. C66 (2010) 1, arXiv:0908.4300]

Pionic contribution to muon $(g-2)$: Basics

- The two-pion contribution to the magnetic moment at LO is

$$a_\mu^{\pi\pi,\text{LO}} = \frac{\alpha^2 m_\mu^2}{12\pi^2}\int_{t_+}^{\infty}\frac{dt}{t}\,K(t)\,\beta_\pi^3(t)\,|F(t)|^2(1+\frac{\alpha}{\pi}\,\eta_\pi(t)),$$

where, $t_+ = 4m_\pi^2$, $\beta_\pi(t) = (1-t_+/t)^{1/2}$ and

$$K(t) = \int_0^1 du(1-u)u^2(t-u+m_\mu^2u^2)^{-1}$$

- The LO contribution does not contain any vacuum polarization effects but include one photon FSR effect. The modulus $|F(t)|$ is extracted from the data by removing the vacuum polarization effect.

- The two-pion contribution to the magnetic moment at LO is

$$a_\mu^{\pi\pi,\mathrm{LO}} = \frac{\alpha^2 m_\mu^2}{12\pi^2} \int_{t_+}^{\infty} \frac{dt}{t}\, K(t)\, \beta_\pi^3(t)\, |F(t)|^2 (1 + \frac{\alpha}{\pi}\, \eta_\pi(t)),$$

where, $t_+ = 4m_\pi^2$, $\beta_\pi(t) = (1 - t_+/t)^{1/2}$ and

$$K(t) = \int_0^1 du (1-u) u^2 (t - u + m_\mu^2 u^2)^{-1}$$

- The LO contribution does not contain any vacuum polarization effects but include one photon FSR effect. The modulus $|F(t)|$ is extracted from the data by removing the vacuum polarization effect.

Pionic contribution to muon $(g-2)$: Basics

- The two-pion contribution to the magnetic moment at LO is

$$a_\mu^{\pi\pi,\mathrm{LO}} = \frac{\alpha^2 m_\mu^2}{12\pi^2} \int_{t_+}^{\infty} \frac{dt}{t}\, K(t)\, \beta_\pi^3(t)\, |F(t)|^2 (1 + \frac{\alpha}{\pi}\, \eta_\pi(t)),$$

where, $t_+ = 4m_\pi^2$, $\beta_\pi(t) = (1 - t_+/t)^{1/2}$ and

$$K(t) = \int_0^1 du(1-u)u^2(t-u+m_\mu^2 u^2)^{-1}$$

- The LO contribution does not contain any vacuum polarization effects but include one photon FSR effect. The modulus $|F(t)|$ is extracted from the data by removing the vacuum polarization effect.

Low energy contribution to a_μ

Leading Order (LO) two-pion contribution to a_μ from the range $[t_l,\, t_u]$:

$$a_\mu^{\pi\pi,\,\mathrm{LO}}[\sqrt{t_l},\sqrt{t_u}] = \frac{\alpha^2 m_\mu^2}{12\pi^2}\int_{t_l}^{t_u} dt\, K(t)\, \beta_\pi^3(t)\, |F(t)|^2 \left(1+\frac{\alpha}{\pi}\,\eta_\pi(t)\right)$$

Particular values [Davier et al. 2010]

- Threshold region, no data, ChPT fit:

$$a_\mu^{\pi\pi,\,\mathrm{LO}}\,[2m_\pi,\, 0.30\,\mathrm{GeV}] = (0.55 \pm 0.01) \times 10^{-10}$$

- From 0.3 GeV to 0.63 GeV, from combined e^+e^- experiments:

$$a_\mu^{\pi\pi,\,\mathrm{LO}}\,[0.30\,\mathrm{GeV},\, 0.63\,\mathrm{GeV}] = (132.6 \pm 1.3) \times 10^{-10}$$

Problem: is it possible to reduce the error by exploiting the properties of $F(t)$ and using information from other energies?

Low energy contribution to a_μ

Leading Order (LO) two-pion contribution to a_μ from the range $[t_l,\ t_u]$:

$$a_\mu^{\pi\pi,\,\mathrm{LO}}[\sqrt{t_l},\sqrt{t_u}] = \frac{\alpha^2 m_\mu^2}{12\pi^2}\int_{t_l}^{t_u} dt\, K(t)\, \beta_\pi^3(t)\, |F(t)|^2 \left(1 + \frac{\alpha}{\pi}\,\eta_\pi(t)\right)$$

Particular values [Davier et al. 2010]

- Threshold region, no data, ChPT fit:

$$a_\mu^{\pi\pi,\,\mathrm{LO}}\,[2m_\pi,\ 0.30\,\mathrm{GeV}] = (0.55 \pm 0.01) \times 10^{-10}$$

- From 0.3 GeV to 0.63 GeV, from combined e^+e^- experiments:

$$a_\mu^{\pi\pi,\,\mathrm{LO}}\,[0.30\,\mathrm{GeV},\ 0.63\,\mathrm{GeV}] = (132.6 \pm 1.3) \times 10^{-10}$$

Problem: is it possible to reduce the error by exploiting the properties of $F(t)$ and using information from other energies?

Low energy contribution to a_μ

Leading Order (LO) two-pion contribution to a_μ from the range $[t_l,\ t_u]$:

$$a_\mu^{\pi\pi,\,\mathrm{LO}}[\sqrt{t_l},\sqrt{t_u}] = \frac{\alpha^2 m_\mu^2}{12\pi^2}\int_{t_l}^{t_u} dt\, K(t)\,\beta_\pi^3(t)\,|F(t)|^2\left(1+\frac{\alpha}{\pi}\,\eta_\pi(t)\right)$$

Particular values [Davier et al. 2010]

- Threshold region, no data, ChPT fit:

$$a_\mu^{\pi\pi,\,\mathrm{LO}}[2m_\pi,\ 0.30\,\mathrm{GeV}] = (0.55 \pm 0.01)\times 10^{-10}$$

- From 0.3 GeV to 0.63 GeV, from combined e^+e^- experiments:

$$a_\mu^{\pi\pi,\,\mathrm{LO}}[0.30\,\mathrm{GeV},\ 0.63\,\mathrm{GeV}] = (132.6 \pm 1.3)\times 10^{-10}$$

Problem: is it possible to reduce the error by exploiting the properties of $F(t)$ and using information from other energies?

Low energy contribution to a_μ

Leading Order (LO) two-pion contribution to a_μ from the range $[t_l,\ t_u]$:

$$a_\mu^{\pi\pi,\,\mathrm{LO}}[\sqrt{t_l},\sqrt{t_u}] = \frac{\alpha^2 m_\mu^2}{12\pi^2}\int_{t_l}^{t_u} dt\, K(t)\, \beta_\pi^3(t)\, |F(t)|^2 \left(1 + \frac{\alpha}{\pi}\,\eta_\pi(t)\right)$$

Particular values [Davier et al. 2010]

- Threshold region, no data, ChPT fit:

$$a_\mu^{\pi\pi,\,\mathrm{LO}}\,[2m_\pi,\ 0.30\,\mathrm{GeV}] = (0.55 \pm 0.01) \times 10^{-10}$$

- From 0.3 GeV to 0.63 GeV, from combined e^+e^- experiments:

$$a_\mu^{\pi\pi,\,\mathrm{LO}}\,[0.30\,\mathrm{GeV},\ 0.63\,\mathrm{GeV}] = (132.6 \pm 1.3) \times 10^{-10}$$

Problem: is it possible to reduce the error by exploiting the properties of $F(t)$ and using information from other energies?

Low energy contribution to a_μ

Leading Order (LO) two-pion contribution to a_μ from the range $[t_l,\ t_u]$:

$$a_\mu^{\pi\pi,\,\mathrm{LO}}[\sqrt{t_l},\sqrt{t_u}] = \frac{\alpha^2 m_\mu^2}{12\pi^2}\int_{t_l}^{t_u} dt\, K(t)\,\beta_\pi^3(t)\,|F(t)|^2\left(1+\frac{\alpha}{\pi}\,\eta_\pi(t)\right)$$

Particular values [Davier et al. 2010]

- Threshold region, no data, ChPT fit:

$$a_\mu^{\pi\pi,\,\mathrm{LO}}\,[2m_\pi,\ 0.30\,\mathrm{GeV}] = (0.55\pm 0.01)\times 10^{-10}$$

- From 0.3 GeV to 0.63 GeV, from combined e^+e^- experiments:

$$a_\mu^{\pi\pi,\,\mathrm{LO}}\,[0.30\,\mathrm{GeV},\ 0.63\,\mathrm{GeV}] = (132.6\pm 1.3)\times 10^{-10}$$

Problem: is it possible to reduce the error by exploiting the properties of $F(t)$ and using information from other energies?

Low energy contribution to a_μ

Leading Order (LO) two-pion contribution to a_μ from the range $[t_l,\ t_u]$:

$$a_\mu^{\pi\pi,\,\mathrm{LO}}[\sqrt{t_l},\sqrt{t_u}] = \frac{\alpha^2 m_\mu^2}{12\pi^2} \int_{t_l}^{t_u} dt\, K(t)\, \beta_\pi^3(t)\, |F(t)|^2 \left(1 + \frac{\alpha}{\pi}\,\eta_\pi(t)\right)$$

Particular values [Davier et al. 2010]

- Threshold region, no data, ChPT fit:

$$a_\mu^{\pi\pi,\,\mathrm{LO}}\,[2m_\pi,\ 0.30\,\mathrm{GeV}] = (0.55 \pm 0.01) \times 10^{-10}$$

- From 0.3 GeV to 0.63 GeV, from combined e^+e^- experiments:

$$a_\mu^{\pi\pi,\,\mathrm{LO}}\,[0.30\,\mathrm{GeV},\ 0.63\,\mathrm{GeV}] = (132.6 \pm 1.3) \times 10^{-10}$$

Problem: is it possible to reduce the error by exploiting the properties of $F(t)$ and using information from other energies?

Pionic contribution to muon $(g-2)$: ranges

- we determine $a_\mu^{\pi\pi,\mathrm{LO}}$ in the regions $[2m_\mu, 0.30\mathrm{GeV}]$ and $[0.30, 0.63\mathrm{GeV}]$ where the cross section data (and hence $|F(t)|$) is poor
- $|F(t)|$ in the regions $[2m_\mu, 0.30\mathrm{GeV}]$ and $[0.30, 0.63\mathrm{GeV}]$ is derived using measured values of $|F(t)|$ between 0.65 GeV to 0.70 GeV.

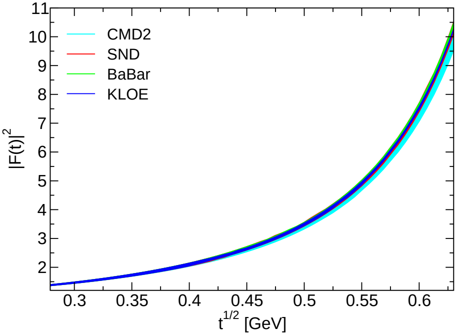

Pionic contribution to muon $(g-2)$: ranges

- we determine $a_\mu^{\pi\pi,\text{LO}}$ in the regions $[2m_\mu, 0.30\text{GeV}]$ and $[0.30, 0.63\text{GeV}]$ where the cross section data (and hence $|F(t)|$) is poor
- $|F(t)|$ in the regions $[2m_\mu, 0.30\text{GeV}]$ and $[0.30, 0.63\text{GeV}]$ is derived using measured values of $|F(t)|$ between 0.65 GeV to 0.70 GeV.

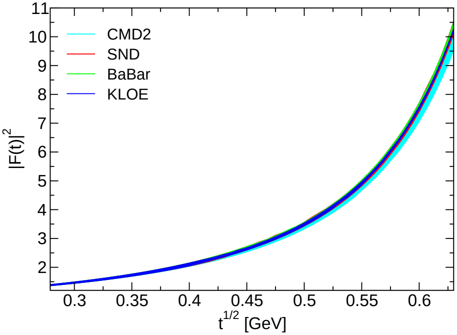

Pionic contribution to muon $(g-2)$: ranges

- we determine $a_\mu^{\pi\pi,\mathrm{LO}}$ in the regions $[2m_\mu, 0.30\mathrm{GeV}]$ and $[0.30, 0.63\mathrm{GeV}]$ where the cross section data (and hence $|F(t)|$) is poor
- $|F(t)|$ in the regions $[2m_\mu, 0.30\mathrm{GeV}]$ and $[0.30, 0.63\mathrm{GeV}]$ is derived using measured values of $|F(t)|$ between 0.65 GeV to 0.70 GeV.

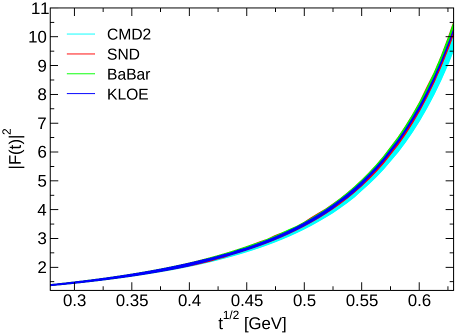

Bounds for experiments as energy of datum is varied

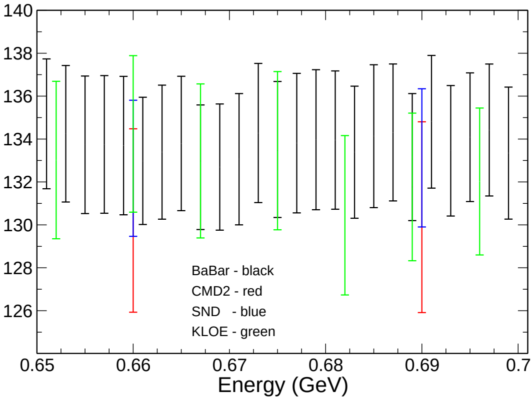

Figure: Allowed intervals of $a_\mu^{\pi\pi,LO}[0.30\mathrm{GeV},\ 0.63\mathrm{GeV}] \times 10^{10}$ using as input the Bern phase and the timelike modulus measured in the region 0.65-0.70 GeV by the e^+e^- experiments.

Bounds for experiments as energy of datum is varied

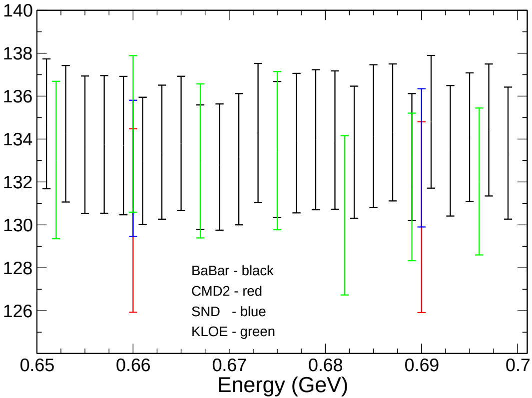

Figure: Allowed intervals of $a_\mu^{\pi\pi,LO}[0.30\mathrm{GeV},\ 0.63\mathrm{GeV}] \times 10^{10}$ using as input the Bern phase and the timelike modulus measured in the region 0.65-0.70 GeV by the e^+e^- experiments.

Optimization procedure

- For central values of the input quantities we obtained very narrow allowed intervals for the output modulus $|F(t)|$ in the range $[t_l, t_u]$ of interest
- To account for the uncertainties, we generated a large sample of data by varying the input quantities (phase, input modulus, spacelike value, charge radius) within their error intervals
- For each point in the sample we computed upper and lower bounds on $|F(t)|$
- We have taken the most conservative bounds, *i.e.* the largest upper bound and the smallest lower bound on $|F(t)|$ from the values obtained with the sample of generated data $\Rightarrow$ a larger allowed interval
- We finally varied the input spacelike and timelike points. Since the analyticity constraints provided by the values at different t must be valid simultaneously, we have taken the "intersection" of the individual allowed ranges, *i.e.* the smallest upper bound and the largest lower bound
- By inserting the upper and lower bounds on $|F(t)|$ into the integral we derived allowed intervals for $a_\mu^{\pi\pi,\,\text{LO}}\,[\sqrt{t_l},\ \sqrt{t_u}]$

Optimization procedure

- For central values of the input quantities we obtained very narrow allowed intervals for the output modulus $|F(t)|$ in the range $[t_l, t_u]$ of interest
- To account for the uncertainties, we generated a large sample of data by varying the input quantities (phase, input modulus, spacelike value, charge radius) within their error intervals
- For each point in the sample we computed upper and lower bounds on $|F(t)|$
- We have taken the most conservative bounds, *i.e.* the largest upper bound and the smallest lower bound on $|F(t)|$ from the values obtained with the sample of generated data $\Rightarrow$ a larger allowed interval
- We finally varied the input spacelike and timelike points. Since the analyticity constraints provided by the values at different t must be valid simultaneously, we have taken the "intersection" of the individual allowed ranges, *i.e.* the smallest upper bound and the largest lower bound
- By inserting the upper and lower bounds on $|F(t)|$ into the integral we derived allowed intervals for $a_\mu^{\pi\pi,\,\mathrm{LO}}[\sqrt{t_l},\ \sqrt{t_u}]$

Optimization procedure

- For central values of the input quantities we obtained very narrow allowed intervals for the output modulus $|F(t)|$ in the range $[t_l, t_u]$ of interest
- To account for the uncertainties, we generated a large sample of data by varying the input quantities (phase, input modulus, spacelike value, charge radius) within their error intervals
- For each point in the sample we computed upper and lower bounds on $|F(t)|$
- We have taken the most conservative bounds, *i.e.* the largest upper bound and the smallest lower bound on $|F(t)|$ from the values obtained with the sample of generated data $\Rightarrow$ a larger allowed interval
- We finally varied the input spacelike and timelike points. Since the analyticity constraints provided by the values at different t must be valid simultaneously, we have taken the "intersection" of the individual allowed ranges, *i.e.* the smallest upper bound and the largest lower bound
- By inserting the upper and lower bounds on $|F(t)|$ into the integral we derived allowed intervals for $a_\mu^{\pi\pi,\,\text{LO}}\,[\sqrt{t_l},\ \sqrt{t_u}]$

Optimization procedure

- For central values of the input quantities we obtained very narrow allowed intervals for the output modulus $|F(t)|$ in the range $[t_l, t_u]$ of interest
- To account for the uncertainties, we generated a large sample of data by varying the input quantities (phase, input modulus, spacelike value, charge radius) within their error intervals
- For each point in the sample we computed upper and lower bounds on $|F(t)|$
- We have taken the most conservative bounds, *i.e.* the largest upper bound and the smallest lower bound on $|F(t)|$ from the values obtained with the sample of generated data $\Rightarrow$ a larger allowed interval
- We finally varied the input spacelike and timelike points. Since the analyticity constraints provided by the values at different t must be valid simultaneously, we have taken the "intersection" of the individual allowed ranges, *i.e.* the smallest upper bound and the largest lower bound
- By inserting the upper and lower bounds on $|F(t)|$ into the integral we derived allowed intervals for $a_\mu^{\pi\pi,\,\text{LO}}\,[\sqrt{t_l},\ \sqrt{t_u}]$

Optimization procedure

- For central values of the input quantities we obtained very narrow allowed intervals for the output modulus $|F(t)|$ in the range $[t_l, t_u]$ of interest
- To account for the uncertainties, we generated a large sample of data by varying the input quantities (phase, input modulus, spacelike value, charge radius) within their error intervals
- For each point in the sample we computed upper and lower bounds on $|F(t)|$
- We have taken the most conservative bounds, *i.e.* the largest upper bound and the smallest lower bound on $|F(t)|$ from the values obtained with the sample of generated data $\Rightarrow$ a larger allowed interval
- We finally varied the input spacelike and timelike points. Since the analyticity constraints provided by the values at different t must be valid simultaneously, we have taken the "intersection" of the individual allowed ranges, *i.e.* the smallest upper bound and the largest lower bound
- By inserting the upper and lower bounds on $|F(t)|$ into the integral we derived allowed intervals for $a_\mu^{\pi\pi,\,\mathrm{LO}}\,[\sqrt{t_l},\ \sqrt{t_u}]$

Optimization procedure

- For central values of the input quantities we obtained very narrow allowed intervals for the output modulus $|F(t)|$ in the range $[t_l, t_u]$ of interest
- To account for the uncertainties, we generated a large sample of data by varying the input quantities (phase, input modulus, spacelike value, charge radius) within their error intervals
- For each point in the sample we computed upper and lower bounds on $|F(t)|$
- We have taken the most conservative bounds, *i.e.* the largest upper bound and the smallest lower bound on $|F(t)|$ from the values obtained with the sample of generated data $\Rightarrow$ a larger allowed interval
- We finally varied the input spacelike and timelike points. Since the analyticity constraints provided by the values at different t must be valid simultaneously, we have taken the "intersection" of the individual allowed ranges, *i.e.* the smallest upper bound and the largest lower bound
- By inserting the upper and lower bounds on $|F(t)|$ into the integral we derived allowed intervals for $a_\mu^{\pi\pi,\,\mathrm{LO}}\,[\sqrt{t_l},\ \sqrt{t_u}]$

Optimization procedure

- For central values of the input quantities we obtained very narrow allowed intervals for the output modulus $|F(t)|$ in the range $[t_l, t_u]$ of interest
- To account for the uncertainties, we generated a large sample of data by varying the input quantities (phase, input modulus, spacelike value, charge radius) within their error intervals
- For each point in the sample we computed upper and lower bounds on $|F(t)|$
- We have taken the most conservative bounds, *i.e.* the largest upper bound and the smallest lower bound on $|F(t)|$ from the values obtained with the sample of generated data $\Rightarrow$ a larger allowed interval
- We finally varied the input spacelike and timelike points. Since the analyticity constraints provided by the values at different t must be valid simultaneously, we have taken the "intersection" of the individual allowed ranges, *i.e.* the smallest upper bound and the largest lower bound
- By inserting the upper and lower bounds on $|F(t)|$ into the integral we derived allowed intervals for $a_\mu^{\pi\pi,\,\mathrm{LO}}\,[\sqrt{t_l},\,\sqrt{t_u}]$

Analysis of the results

- For SND and CMD2 the intervals are rather large and consistent between them
- For BABAR the intervals are narrower and exhibit a moderate variation from point to point
- For KLOE the intervals exhibit a more pronounced variation with the input point

- Taking the intersection is equivalent with combining the central values and errors with a large correlation
- This prescription requires good, consistent input data, which produce narrow allowed intervals with a relatively large common part
- A too small overlap may signal inconsistencies among the input data

- In this analysis we kept all the points, assuming they are all reliable

Analysis of the results

- For SND and CMD2 the intervals are rather large and consistent between them
- For BABAR the intervals are narrower and exhibit a moderate variation from point to point
- For KLOE the intervals exhibit a more pronounced variation with the input point

- Taking the intersection is equivalent with combining the central values and errors with a large correlation
- This prescription requires good, consistent input data, which produce narrow allowed intervals with a relatively large common part
- A too small overlap may signal inconsistencies among the input data

- In this analysis we kept all the points, assuming they are all reliable

Analysis of the results

- For SND and CMD2 the intervals are rather large and consistent between them
- For BABAR the intervals are narrower and exhibit a moderate variation from point to point
- For KLOE the intervals exhibit a more pronounced variation with the input point

- Taking the intersection is equivalent with combining the central values and errors with a large correlation
- This prescription requires good, consistent input data, which produce narrow allowed intervals with a relatively large common part
- A too small overlap may signal inconsistencies among the input data

- In this analysis we kept all the points, assuming they are all reliable

Analysis of the results

- For SND and CMD2 the intervals are rather large and consistent between them
- For BABAR the intervals are narrower and exhibit a moderate variation from point to point
- For KLOE the intervals exhibit a more pronounced variation with the input point

- Taking the intersection is equivalent with combining the central values and errors with a large correlation
- This prescription requires good, consistent input data, which produce narrow allowed intervals with a relatively large common part
- A too small overlap may signal inconsistencies among the input data

- In this analysis we kept all the points, assuming they are all reliable

Analysis of the results

- For SND and CMD2 the intervals are rather large and consistent between them
- For BABAR the intervals are narrower and exhibit a moderate variation from point to point
- For KLOE the intervals exhibit a more pronounced variation with the input point

- Taking the intersection is equivalent with combining the central values and errors with a large correlation
- This prescription requires good, consistent input data, which produce narrow allowed intervals with a relatively large common part
- A too small overlap may signal inconsistencies among the input data

- In this analysis we kept all the points, assuming they are all reliable

Analysis of the results

- For SND and CMD2 the intervals are rather large and consistent between them
- For BABAR the intervals are narrower and exhibit a moderate variation from point to point
- For KLOE the intervals exhibit a more pronounced variation with the input point

- Taking the intersection is equivalent with combining the central values and errors with a large correlation
- This prescription requires good, consistent input data, which produce narrow allowed intervals with a relatively large common part
- A too small overlap may signal inconsistencies among the input data

- In this analysis we kept all the points, assuming they are all reliable

Analysis of the results

- For SND and CMD2 the intervals are rather large and consistent between them
- For BABAR the intervals are narrower and exhibit a moderate variation from point to point
- For KLOE the intervals exhibit a more pronounced variation with the input point

- Taking the intersection is equivalent with combining the central values and errors with a large correlation
- This prescription requires good, consistent input data, which produce narrow allowed intervals with a relatively large common part
- A too small overlap may signal inconsistencies among the input data

- In this analysis we kept all the points, assuming they are all reliable

Analysis of the results

- For SND and CMD2 the intervals are rather large and consistent between them
- For BABAR the intervals are narrower and exhibit a moderate variation from point to point
- For KLOE the intervals exhibit a more pronounced variation with the input point

- Taking the intersection is equivalent with combining the central values and errors with a large correlation
- This prescription requires good, consistent input data, which produce narrow allowed intervals with a relatively large common part
- A too small overlap may signal inconsistencies among the input data

- In this analysis we kept all the points, assuming they are all reliable

Pionic contribution to muon $(g-2)$: results

Table: Central values and errors for the quantity $a_\mu^{\pi\pi,LO}[2m_\pi,\, 0.30\mathrm{GeV}] \times 10^{10}$ obtained from the bounds on $|F(t)|$ calculated with input from the four e^+e^- experiments.

	Bern phase	Madrid phase
CMD2 06	0.5528 ± 0.0089	0.5527 ± 0.0092
SND 06	0.5532 ± 0.0083	0.5530 ± 0.0086
BABAR 09	0.5534 ± 0.0080	0.5533 ± 0.0083
KLOE 13	0.5531 ± 0.0080	0.5530 ± 0.0084

Table: Central values and errors for the quantity $a_\mu^{\pi\pi,LO}[0.30\mathrm{GeV},\, 0.63\mathrm{GeV}] \times 10^{10}$ obtained from the bounds on $|F(t)|$ calculated with input from the four e^+e^- experiments.

	Bern phase	Madrid phase
CMD2 06	130.531 ± 3.955	129.739 ± 4.545
SND 06	132.775 ± 2.862	132.313 ± 2.759
BABAR 09	133.732 ± 1.761	133.484 ± 1.461
KLOE 13	132.380 ± 1.721	132.086 ± 1.451

Pionic contribution to muon $(g-2)$: results

Table: Central values and errors for the quantity $a_\mu^{\pi\pi,LO}\,[2m_\pi,\ 0.30\mathrm{GeV}] \times 10^{10}$ obtained from the bounds on $|F(t)|$ calculated with input from the four e^+e^- experiments.

	Bern phase	Madrid phase
CMD2 06	0.5528 $\pm$ 0.0089	0.5527 $\pm$ 0.0092
SND 06	0.5532 $\pm$ 0.0083	0.5530 $\pm$ 0.0086
BABAR 09	0.5534 $\pm$ 0.0080	0.5533 $\pm$ 0.0083
KLOE 13	0.5531 $\pm$ 0.0080	0.5530 $\pm$ 0.0084

Table: Central values and errors for the quantity $a_\mu^{\pi\pi,LO}\,[0.30\mathrm{GeV},\ 0.63\mathrm{GeV}] \times 10^{10}$ obtained from the bounds on $|F(t)|$ calculated with input from the four e^+e^- experiments.

	Bern phase	Madrid phase
CMD2 06	130.531 $\pm$ 3.955	129.739 $\pm$ 4.545
SND 06	132.775 $\pm$ 2.862	132.313 $\pm$ 2.759
BABAR 09	133.732 $\pm$ 1.761	133.484 $\pm$ 1.461
KLOE 13	132.380 $\pm$ 1.721	132.086 $\pm$ 1.451

Pionic contribution to muon $(g-2)$: results

Table: Central values and errors for the quantity $a_\mu^{\pi\pi,LO}\,[2m_\pi,\ 0.30\mathrm{GeV}] \times 10^{10}$ obtained from the bounds on $|F(t)|$ calculated with input from the four e^+e^- experiments.

	Bern phase	Madrid phase
CMD2 06	0.5528 ± 0.0089	0.5527 ± 0.0092
SND 06	0.5532 ± 0.0083	0.5530 ± 0.0086
BABAR 09	0.5534 ± 0.0080	0.5533 ± 0.0083
KLOE 13	0.5531 ± 0.0080	0.5530 ± 0.0084

Table: Central values and errors for the quantity $a_\mu^{\pi\pi,LO}\,[0.30\mathrm{GeV},\ 0.63\mathrm{GeV}] \times 10^{10}$ obtained from the bounds on $|F(t)|$ calculated with input from the four e^+e^- experiments.

	Bern phase	Madrid phase
CMD2 06	130.531 ± 3.955	129.739 ± 4.545
SND 06	132.775 ± 2.862	132.313 ± 2.759
BABAR 09	133.732 ± 1.761	133.484 ± 1.461
KLOE 13	132.380 ± 1.721	132.086 ± 1.451

Pionic contribution to muon $(g-2)$: summary

After combining four experiments and two phases

$$a_\mu^{\pi\pi,\text{LO}}[2m_\pi,\, 0.30\text{GeV}] = (0.553 \pm 0.004) \times 10^{-10}, \quad (1)$$

and

$$a_\mu^{\pi\pi,\text{LO}}[0.30\text{GeV},\, 0.63\text{GeV}] = (132.703 \pm 1.018) \times 10^{-10}. \quad (2)$$

- $a_\mu^{\pi\pi,\text{LO}}[2m_\pi,\, 0.30\text{GeV}] = (0.55 \pm 0.01) \times 10^{-10}$
  $a_\mu^{\pi\pi,\text{LO}}[0.30\text{GeV},\, 0.63\text{GeV}] = (132.6 \pm 1.3) \times 10^{-10}$ [Davier *et. al* 2010]
- $a_\mu^{\pi\pi,\text{LO}}[0.30\text{GeV},\, 0.63\text{GeV}] = (133.877 \pm 1.472) \times 10^{-10}$ [BABAR]
- remarkable consistency of BABAR data with the analyticity constraints
- by combining the direct integration of the BABAR data below 0.63 GeV with our independent determination based on data from higher energies for the other three experiments we obtain

$$a_\mu^{\pi\pi,\text{LO}}[0.30\text{GeV},\, 0.63\text{GeV}] = (133.083 \pm 0.837) \times 10^{-10} \quad (3)$$

Pionic contribution to muon $(g-2)$: summary

After combining four experiments and two phases

$$a_\mu^{\pi\pi,\text{LO}}[2m_\pi,\ 0.30\text{GeV}] = (0.553 \pm 0.004) \times 10^{-10}, \tag{1}$$

and

$$a_\mu^{\pi\pi,\text{LO}}[0.30\text{GeV},\ 0.63\text{GeV}] = (132.703 \pm 1.018) \times 10^{-10}. \tag{2}$$

- $a_\mu^{\pi\pi,\text{LO}}[2m_\pi,\ 0.30\text{GeV}] = (0.55 \pm 0.01) \times 10^{-10}$
  $a_\mu^{\pi\pi,\text{LO}}[0.30\text{GeV},\ 0.63\text{GeV}] = (132.6 \pm 1.3) \times 10^{-10}$ [Davier *et. al* 2010]
- $a_\mu^{\pi\pi,\text{LO}}[0.30\text{GeV},\ 0.63\text{GeV}] = (133.877 \pm 1.472) \times 10^{-10}$ [BABAR]
- remarkable consistency of BABAR data with the analyticity constraints
- by combining the direct integration of the BABAR data below 0.63 GeV with our independent determination based on data from higher energies for the other three experiments we obtain

$$a_\mu^{\pi\pi,\text{LO}}[0.30\text{GeV},\ 0.63\text{GeV}] = (133.083 \pm 0.837) \times 10^{-10} \tag{3}$$

Pionic contribution to muon $(g-2)$: summary

After combining four experiments and two phases

$$a_\mu^{\pi\pi,\text{LO}}\,[2m_\pi,\,0.30\text{GeV}] = (0.553 \pm 0.004) \times 10^{-10}, \tag{1}$$

and

$$a_\mu^{\pi\pi,\text{LO}}\,[0.30\text{GeV},\,0.63\text{GeV}] = (132.703 \pm 1.018) \times 10^{-10}. \tag{2}$$

- $a_\mu^{\pi\pi,\text{LO}}\,[2m_\pi,\,0.30\text{GeV}] = (0.55 \pm 0.01) \times 10^{-10}$
  $a_\mu^{\pi\pi,\text{LO}}\,[0.30\text{GeV},\,0.63\text{GeV}] = (132.6 \pm 1.3) \times 10^{-10}$ [Davier *et. al* 2010]
- $a_\mu^{\pi\pi,\text{LO}}\,[0.30\text{GeV},\,0.63\text{GeV}] = (133.877 \pm 1.472) \times 10^{-10}$ [BABAR]
- remarkable consistency of BABAR data with the analyticity constraints
- by combining the direct integration of the BABAR data below 0.63 GeV with our independent determination based on data from higher energies for the other three experiments we obtain

$$a_\mu^{\pi\pi,\text{LO}}\,[0.30\text{GeV},\,0.63\text{GeV}] = (133.083 \pm 0.837) \times 10^{-10} \tag{3}$$

Pionic contribution to muon $(g-2)$: summary

After combining four experiments and two phases

$$a_\mu^{\pi\pi,\text{LO}}\,[2m_\pi,\,0.30\text{GeV}] = (0.553 \pm 0.004) \times 10^{-10}, \tag{1}$$

and

$$a_\mu^{\pi\pi,\text{LO}}\,[0.30\text{GeV},\,0.63\text{GeV}] = (132.703 \pm 1.018) \times 10^{-10}. \tag{2}$$

- $a_\mu^{\pi\pi,\text{LO}}\,[2m_\pi,\,0.30\text{GeV}] = (0.55 \pm 0.01) \times 10^{-10}$
  $a_\mu^{\pi\pi,\text{LO}}\,[0.30\text{GeV},\,0.63\text{GeV}] = (132.6 \pm 1.3) \times 10^{-10}$ [Davier *et. al* 2010]
- $a_\mu^{\pi\pi,\text{LO}}\,[0.30\text{GeV},\,0.63\text{GeV}] = (133.877 \pm 1.472) \times 10^{-10}$ [BABAR]
- remarkable consistency of BABAR data with the analyticity constraints
- by combining the direct integration of the BABAR data below 0.63 GeV with our independent determination based on data from higher energies for the other three experiments we obtain

$$a_\mu^{\pi\pi,\text{LO}}\,[0.30\text{GeV},\,0.63\text{GeV}] = (133.083 \pm 0.837) \times 10^{-10} \tag{3}$$

Pionic contribution to muon $(g-2)$: summary

After combining four experiments and two phases

$$a_\mu^{\pi\pi,\text{LO}}\,[2m_\pi,\, 0.30\text{GeV}] = (0.553 \pm 0.004) \times 10^{-10}, \tag{1}$$

and

$$a_\mu^{\pi\pi,\text{LO}}\,[0.30\text{GeV},\, 0.63\text{GeV}] = (132.703 \pm 1.018) \times 10^{-10}. \tag{2}$$

- $a_\mu^{\pi\pi,\text{LO}}\,[2m_\pi,\, 0.30\text{GeV}] = (0.55 \pm 0.01) \times 10^{-10}$
  $a_\mu^{\pi\pi,\text{LO}}\,[0.30\text{GeV},\, 0.63\text{GeV}] = (132.6 \pm 1.3) \times 10^{-10}$ [Davier *et. al* 2010]
- $a_\mu^{\pi\pi,\text{LO}}\,[0.30\text{GeV},\, 0.63\text{GeV}] = (133.877 \pm 1.472) \times 10^{-10}$ [BABAR]
- remarkable consistency of BABAR data with the analyticity constraints
- by combining the direct integration of the BABAR data below 0.63 GeV with our independent determination based on data from higher energies for the other three experiments we obtain

$$a_\mu^{\pi\pi,\text{LO}}\,[0.30\text{GeV},\, 0.63\text{GeV}] = (133.083 \pm 0.837) \times 10^{-10} \tag{3}$$

Pionic contribution to muon $(g-2)$: summary

After combining four experiments and two phases

$$a_\mu^{\pi\pi,\text{LO}}\,[2m_\pi,\,0.30\text{GeV}] = (0.553 \pm 0.004) \times 10^{-10}, \tag{1}$$

and

$$a_\mu^{\pi\pi,\text{LO}}\,[0.30\text{GeV},\,0.63\text{GeV}] = (132.703 \pm 1.018) \times 10^{-10}. \tag{2}$$

- $a_\mu^{\pi\pi,\text{LO}}\,[2m_\pi,\,0.30\text{GeV}] = (0.55 \pm 0.01) \times 10^{-10}$
  $a_\mu^{\pi\pi,\text{LO}}\,[0.30\text{GeV},\,0.63\text{GeV}] = (132.6 \pm 1.3) \times 10^{-10}$ [Davier *et. al* 2010]
- $a_\mu^{\pi\pi,\text{LO}}\,[0.30\text{GeV},\,0.63\text{GeV}] = (133.877 \pm 1.472) \times 10^{-10}$ [BABAR]
- remarkable consistency of BABAR data with the analyticity constraints
- by combining the direct integration of the BABAR data below 0.63 GeV with our independent determination based on data from higher energies for the other three experiments we obtain

$$a_\mu^{\pi\pi,\text{LO}}\,[0.30\text{GeV},\,0.63\text{GeV}] = (133.083 \pm 0.837) \times 10^{-10} \tag{3}$$

Pionic contribution to muon $(g-2)$: summary

After combining four experiments and two phases

$$a_\mu^{\pi\pi,\text{LO}}\,[2m_\pi,\,0.30\text{GeV}] = (0.553 \pm 0.004)\times 10^{-10}, \quad (1)$$

and

$$a_\mu^{\pi\pi,\text{LO}}\,[0.30\text{GeV},\,0.63\text{GeV}] = (132.703 \pm 1.018)\times 10^{-10}. \quad (2)$$

- $a_\mu^{\pi\pi,\text{LO}}\,[2m_\pi,\,0.30\text{GeV}] = (0.55 \pm 0.01)\times 10^{-10}$
  $a_\mu^{\pi\pi,\text{LO}}\,[0.30\text{GeV},\,0.63\text{GeV}] = (132.6 \pm 1.3)\times 10^{-10}$ [Davier *et. al* 2010]
- $a_\mu^{\pi\pi,\text{LO}}\,[0.30\text{GeV},\,0.63\text{GeV}] = (133.877 \pm 1.472)\times 10^{-10}$ [BABAR]
- remarkable consistency of BABAR data with the analyticity constraints
- by combining the direct integration of the BABAR data below 0.63 GeV with our independent determination based on data from higher energies for the other three experiments we obtain

$$a_\mu^{\pi\pi,\text{LO}}\,[0.30\text{GeV},\,0.63\text{GeV}] = (133.083 \pm 0.837)\times 10^{-10} \quad (3)$$

Pionic contribution to muon $(g-2)$: Conclusion

- We have devised a non-perturbative analytic tool for improving the determination of the pionic contribution to muon $(g-2)$
- This model independent approach reduces the error by $\delta_\mu^{\pi,\pi} = 5 \times 10^{-11}$
- With improved input from low and intermediate energies the uncertainty in the hadronic part of the muon anomaly can be further reduced
- Calls for more precise experimental information in the low energy region and also the region where the main contribution to the $(g-2)$ comes from
- Extension of our work to τ-decay data in progress

Pionic contribution to muon $(g-2)$: Conclusion

- We have devised a non-perturbative analytic tool for improving the determination of the pionic contribution to muon $(g-2)$
- This model independent approach reduces the error by $\delta_{\mu}^{\pi,\pi} = 5 \times 10^{-11}$
- With improved input from low and intermediate energies the uncertainty in the hadronic part of the muon anomaly can be further reduced
- Calls for more precise experimental information in the low energy region and also the region where the main contribution to the $(g-2)$ comes from
- Extension of our work to τ-decay data in progress

Pionic contribution to muon $(g-2)$: Conclusion

- We have devised a non-perturbative analytic tool for improving the determination of the pionic contribution to muon $(g-2)$
- This model independent approach reduces the error by $\delta_{\mu}^{\pi,\pi} = 5 \times 10^{-11}$
- With improved input from low and intermediate energies the uncertainty in the hadronic part of the muon anomaly can be further reduced
- Calls for more precise experimental information in the low energy region and also the region where the main contribution to the $(g-2)$ comes from
- Extension of our work to τ-decay data in progress

Pionic contribution to muon $(g-2)$: Conclusion

- We have devised a non-perturbative analytic tool for improving the determination of the pionic contribution to muon $(g-2)$
- This model independent approach reduces the error by $\delta_{\mu}^{\pi,\pi} = 5 \times 10^{-11}$
- With improved input from low and intermediate energies the uncertainty in the hadronic part of the muon anomaly can be further reduced
- Calls for more precise experimental information in the low energy region and also the region where the main contribution to the $(g-2)$ comes from
- Extension of our work to τ-decay data in progress

Pionic contribution to muon $(g-2)$: Conclusion

- We have devised a non-perturbative analytic tool for improving the determination of the pionic contribution to muon $(g-2)$
- This model independent approach reduces the error by $\delta_{\mu}^{\pi,\pi} = 5 \times 10^{-11}$
- With improved input from low and intermediate energies the uncertainty in the hadronic part of the muon anomaly can be further reduced
- Calls for more precise experimental information in the low energy region and also the region where the main contribution to the $(g-2)$ comes from
- Extension of our work to τ-decay data in progress

Pionic contribution to muon $(g-2)$: Conclusion

- We have devised a non-perturbative analytic tool for improving the determination of the pionic contribution to muon $(g-2)$
- This model independent approach reduces the error by $\delta_{\mu}^{\pi,\pi} = 5 \times 10^{-11}$
- With improved input from low and intermediate energies the uncertainty in the hadronic part of the muon anomaly can be further reduced
- Calls for more precise experimental information in the low energy region and also the region where the main contribution to the $(g-2)$ comes from
- Extension of our work to τ-decay data in progress

Statistical interpretation of the results

- Start with prior distributions of the inputs – phase (uniform distribution), spacelike data (gaussian), radius (uniform), and timelike data in the stable region (gaussian).
- Assume the priors to be identical to the posterior distribution in our case.
- First keep the timelike value fixed and vary the inputs. All the inputs simultaneously varied.
- Enlarge the bounds by the corresponding error. This way bounds are valid to a certain confidence.
- The above is done for a fixed timelike input. Then we vary the timelike input, repeat the procedure for several timelike inputs at different points (in the stable region) and combine the resulting bounds.

Statistical interpretation of the results

- Start with prior distributions of the inputs – phase (uniform distribution), spacelike data (gaussian), radius (uniform), and timelike data in the stable region (gaussian).
- Assume the priors to be identical to the posterior distribution in our case.
- First keep the timelike value fixed and vary the inputs. All the inputs simultaneously varied.
- Enlarge the bounds by the corresponding error. This way bounds are valid to a certain confidence.
- The above is done for a fixed timelike input. Then we vary the timelike input, repeat the procedure for several timelike inputs at different points (in the stable region) and combine the resulting bounds.

Statistical interpretation of the results

- Start with prior distributions of the inputs – phase (uniform distribution), spacelike data (gaussian), radius (uniform), and timelike data in the stable region (gaussian).
- Assume the priors to be identical to the posterior distribution in our case.
- First keep the timelike value fixed and vary the inputs. All the inputs simultaneously varied.
- Enlarge the bounds by the corresponding error. This way bounds are valid to a certain confidence.
- The above is done for a fixed timelike input. Then we vary the timelike input, repeat the procedure for several timelike inputs at different points (in the stable region) and combine the resulting bounds.

Statistical interpretation of the results

- Start with prior distributions of the inputs – phase (uniform distribution), spacelike data (gaussian), radius (uniform), and timelike data in the stable region (gaussian).
- Assume the priors to be identical to the posterior distribution in our case.
- First keep the timelike value fixed and vary the inputs. All the inputs simultaneously varied.
- Enlarge the bounds by the corresponding error. This way bounds are valid to a certain confidence.
- The above is done for a fixed timelike input. Then we vary the timelike input, repeat the procedure for several timelike inputs at different points (in the stable region) and combine the resulting bounds.

Statistical interpretation of the results

- Start with prior distributions of the inputs – phase (uniform distribution), spacelike data (gaussian), radius (uniform), and timelike data in the stable region (gaussian).
- Assume the priors to be identical to the posterior distribution in our case.
- First keep the timelike value fixed and vary the inputs. All the inputs simultaneously varied.
- Enlarge the bounds by the corresponding error. This way bounds are valid to a certain confidence.
- The above is done for a fixed timelike input. Then we vary the timelike input, repeat the procedure for several timelike inputs at different points (in the stable region) and combine the resulting bounds.

Statistical interpretation of the results

- Start with prior distributions of the inputs – phase (uniform distribution), spacelike data (gaussian), radius (uniform), and timelike data in the stable region (gaussian).
- Assume the priors to be identical to the posterior distribution in our case.
- First keep the timelike value fixed and vary the inputs. All the inputs simultaneously varied.
- Enlarge the bounds by the corresponding error. This way bounds are valid to a certain confidence.
- The above is done for a fixed timelike input. Then we vary the timelike input, repeat the procedure for several timelike inputs at different points (in the stable region) and combine the resulting bounds.

Statistics continue

- Statistical approach to perform the above analysis –
  - Denote by δ_i the error on the bound B_i at a certain point due to the timelike input i.
  - Consider the error propagation to calculate a covariance matrix (from PDG) for the bounds.

$$U_{ij} = \Sigma_{k,l} \frac{\partial \eta_i}{\partial \theta_k} \frac{\partial \eta_j}{\partial \theta_l} |_{\hat{\theta}} V_{kl}$$

    V_{kl}, $k, l = 1, \ldots, n$ is the experimental correlation matrix.
  - From the matrix U_{ij} and the central values B_i, one can obtain the average and the corresponding error δ_i of the bounds at a fixed point. The bounds increased by the error will be represent the bounds at @ 68% confidence.
  - Work in progress and results coming up soon

Statistics continue

- Statistical approach to perform the above analysis –
  - Denote by δ_i the error on the bound B_i at a certain point due to the timelike input i.
  - Consider the error propagation to calculate a covariance matrix (from PDG) for the bounds.

$$U_{ij} = \Sigma_{k,l} \frac{\partial \eta_i}{\partial \theta_k} \frac{\partial \eta_j}{\partial \theta_l} |_{\hat{\theta}} V_{kl}$$

    $V_{kl},\, k, l = 1, \ldots, n$ is the experimental correlation matrix.
  - From the matrix U_{ij} and the central values B_i, one can obtain the average and the corresponding error δ_i of the bounds at a fixed point. The bounds increased by the error will be represent the bounds at @ 68% confidence.
  - Work in progress and results coming up soon

Statistics continue

- Statistical approach to perform the above analysis –
  - Denote by δ_i the error on the bound B_i at a certain point due to the timelike input i.
  - Consider the error propagation to calculate a covariance matrix (from PDG) for the bounds.
$$U_{ij} = \Sigma_{k,l} \frac{\partial \eta_i}{\partial \theta_k} \frac{\partial \eta_j}{\partial \theta_l} |_{\hat{\theta}} V_{kl}$$
    V_{kl}, $k, l = 1, \ldots, n$ is the experimental correlation matrix.
  - From the matrix U_{ij} and the central values B_i, one can obtain the average and the corresponding error δ_i of the bounds at a fixed point. The bounds increased by the error will be represent the bounds at @ 68% confidence.
  - Work in progress and results coming up soon

Statistics continue

- Statistical approach to perform the above analysis –
  - Denote by δ_i the error on the bound B_i at a certain point due to the timelike input i.
  - Consider the error propagation to calculate a covariance matrix (from PDG) for the bounds.

    $$U_{ij} = \Sigma_{k,l} \frac{\partial \eta_i}{\partial \theta_k} \frac{\partial \eta_j}{\partial \theta_l} |_{\hat{\theta}} V_{kl}$$

    $V_{kl}, k, l = 1, ..., n$ is the experimental correlation matrix.
  - From the matrix U_{ij} and the central values B_i, one can obtain the average and the corresponding error δ_i of the bounds at a fixed point. The bounds increased by the error will be represent the bounds at @ 68% confidence.
  - Work in progress and results coming up soon

Statistics continue

- Statistical approach to perform the above analysis –
  - Denote by δ_i the error on the bound B_i at a certain point due to the timelike input i.
  - Consider the error propagation to calculate a covariance matrix (from PDG) for the bounds.

$$U_{ij} = \Sigma_{k,l} \frac{\partial \eta_i}{\partial \theta_k} \frac{\partial \eta_j}{\partial \theta_l} |_{\hat{\theta}} V_{kl}$$

    $V_{kl}, k, l = 1, ..., n$ is the experimental correlation matrix.
  - From the matrix U_{ij} and the central values B_i, one can obtain the average and the corresponding error δ_i of the bounds at a fixed point. The bounds increased by the error will be represent the bounds at @ 68% confidence.
  - Work in progress and results coming up soon

Statistics continue

- Statistical approach to perform the above analysis –
  - Denote by δ_i the error on the bound B_i at a certain point due to the timelike input i.
  - Consider the error propagation to calculate a covariance matrix (from PDG) for the bounds.

    $$U_{ij} = \Sigma_{k,l} \frac{\partial \eta_i}{\partial \theta_k} \frac{\partial \eta_j}{\partial \theta_l} |_{\hat{\theta}} V_{kl}$$

    $V_{kl}, k, l = 1, \ldots, n$ is the experimental correlation matrix.
  - From the matrix U_{ij} and the central values B_i, one can obtain the average and the corresponding error δ_i of the bounds at a fixed point. The bounds increased by the error will be represent the bounds at @ 68% confidence.
  - Work in progress and results coming up soon

Conclusions and Outlook

Conclusions

- Worked the Meiman problem to logical extremes
- Used high precision inputs from a variety of sources
- Phase information
- Spacelike information
- High Precision modulus measurements
- Computed bounds on modulus in low energy region
- Computed bounds on shape parameters
- Obtained excellent evaluation of pionic contribution to muon $(g-2)$ confirming central values with reduced error of prior determinations

Conclusions

- Worked the Meiman problem to logical extremes
- Used high precision inputs from a variety of sources
- Phase information
- Spacelike information
- High Precision modulus measurements
- Computed bounds on modulus in low energy region
- Computed bounds on shape parameters
- Obtained excellent evaluation of pionic contribution to muon $(g-2)$ confirming central values with reduced error of prior determinations

Conclusions

- Worked the Meiman problem to logical extremes
- Used high precision inputs from a variety of sources
- Phase information
- Spacelike information
- High Precision modulus measurements
- Computed bounds on modulus in low energy region
- Computed bounds on shape parameters
- Obtained excellent evaluation of pionic contribution to muon $(g-2)$ confirming central values with reduced error of prior determinations

Conclusions

- Worked the Meiman problem to logical extremes
- Used high precision inputs from a variety of sources
- Phase information
- Spacelike information
- High Precision modulus measurements
- Computed bounds on modulus in low energy region
- Computed bounds on shape parameters
- Obtained excellent evaluation of pionic contribution to muon $(g-2)$ confirming central values with reduced error of prior determinations

Conclusions

- Worked the Meiman problem to logical extremes
- Used high precision inputs from a variety of sources
- Phase information
- Spacelike information
- High Precision modulus measurements
- Computed bounds on modulus in low energy region
- Computed bounds on shape parameters
- Obtained excellent evaluation of pionic contribution to muon $(g-2)$ confirming central values with reduced error of prior determinations

Conclusions

- Worked the Meiman problem to logical extremes
- Used high precision inputs from a variety of sources
- Phase information
- Spacelike information
- High Precision modulus measurements
- Computed bounds on modulus in low energy region
- Computed bounds on shape parameters
- Obtained excellent evaluation of pionic contribution to muon $(g-2)$ confirming central values with reduced error of prior determinations

Conclusions

- Worked the Meiman problem to logical extremes
- Used high precision inputs from a variety of sources
- Phase information
- Spacelike information
- High Precision modulus measurements
- Computed bounds on modulus in low energy region
- Computed bounds on shape parameters
- Obtained excellent evaluation of pionic contribution to muon $(g-2)$ confirming central values with reduced error of prior determinations

Conclusions

- Worked the Meiman problem to logical extremes
- Used high precision inputs from a variety of sources
- Phase information
- Spacelike information
- High Precision modulus measurements
- Computed bounds on modulus in low energy region
- Computed bounds on shape parameters
- Obtained excellent evaluation of pionic contribution to muon $(g-2)$ confirming central values with reduced error of prior determinations

Conclusions

- Worked the Meiman problem to logical extremes
- Used high precision inputs from a variety of sources
- Phase information
- Spacelike information
- High Precision modulus measurements
- Computed bounds on modulus in low energy region
- Computed bounds on shape parameters
- Obtained excellent evaluation of pionic contribution to muon $(g-2)$ confirming central values with reduced error of prior determinations

Outlook

- Meiman problem proved to be a very useful tool
- Extension to data from τ-decays
- Other effects such as $\rho - \gamma$ mixing need to be studied
- Combining of results from different experiments
- Role of correlations need to be examined and elucidated upon
- Statistical analysis work in progress

Outlook

- Meiman problem proved to be a very useful tool
- Extension to data from τ-decays
- Other effects such as $\rho - \gamma$ mixing need to be studied
- Combining of results from different experiments
- Role of correlations need to be examined and elucidated upon
- Statistical analysis work in progress

Outlook

- Meiman problem proved to be a very useful tool
- Extension to data from τ-decays
- Other effects such as $\rho - \gamma$ mixing need to be studied
- Combining of results from different experiments
- Role of correlations need to be examined and elucidated upon
- Statistical analysis work in progress

Outlook

- Meiman problem proved to be a very useful tool
- Extension to data from τ-decays
- Other effects such as $\rho - \gamma$ mixing need to be studied
- Combining of results from different experiments
- Role of correlations need to be examined and elucidated upon
- Statistical analysis work in progress

Outlook

- Meiman problem proved to be a very useful tool
- Extension to data from τ-decays
- Other effects such as $\rho - \gamma$ mixing need to be studied
- Combining of results from different experiments
- Role of correlations need to be examined and elucidated upon
- Statistical analysis work in progress

Outlook

- Meiman problem proved to be a very useful tool
- Extension to data from τ-decays
- Other effects such as $\rho - \gamma$ mixing need to be studied
- Combining of results from different experiments
- Role of correlations need to be examined and elucidated upon
- Statistical analysis work in progress